LBL-155
c.2

LOW ENERGY ELECTRON DIFFRACTION STUDIES OF INSULATING SINGLE CRYSTAL SURFACES

Theodore M. French
(Ph.D. thesis)

October 1971

AEC Contract No. W-7405-eng-48

TWO-WEEK LOAN COPY

This is a Library Circulating Copy
which may be borrowed for two weeks.
For a personal retention copy, call
Tech. Info. Division, Ext. 5545

LBL-155
c.2

DISCLAIMER

This document was prepared as an account of work sponsored by the United States Government. While this document is believed to contain correct information, neither the United States Government nor any agency thereof, nor the Regents of the University of California, nor any of their employees, makes any warranty, express or implied, or assumes any legal responsibility for the accuracy, completeness, or usefulness of any information, apparatus, product, or process disclosed, or represents that its use would not infringe privately owned rights. Reference herein to any specific commercial product, process, or service by its trade name, trademark, manufacturer, or otherwise, does not necessarily constitute or imply its endorsement, recommendation, or favoring by the United States Government or any agency thereof, or the Regents of the University of California. The views and opinions of authors expressed herein do not necessarily state or reflect those of the United States Government or any agency thereof or the Regents of the University of California.

LOW ENERGY ELECTRON DIFFRACTION STUDIES OF INSULATING SINGLE CRYSTAL SURFACES

Contents

Abstract v

I. Introduction 1

II. The Diffraction of Low Energy Electrons from Single Crystal Surfaces. 3

III. Preparation of Single Crystal Samples for LEED Studies . . . 8

1. Alumina (Al_2O_3). 8

2. Alkali Halides 9

3. Silicon Oxide (quartz) 10

IV. Elimination of Surface Charge at Insulator Surfaces During LEED Studies 11

V. The Low Energy Electron Diffraction Experiment 15

VI. Intensity Data. 17

VII. Temperature Dependence of Diffraction Beam Intensities . . 21

VIII. The Decomposition of Alkali-Halide Crystal Surfaces in the Electron Beam. 25

IX. Surface Chemistry of Alumina. 31

X. The Surface Chemistry of SiO_2 (Quartz) 40

XI. The Surface Chemistry of NaF, LiF, and NaCl (100) Face. . . 41

XII. The Effect of the Incident Electron Beam on the Surface of α-Alumina 42

Acknowledgments. 46

References 47

LOW ENERGY ELECTRON DIFFRACTION STUDIES OF INSULATING SINGLE CRYSTAL SURFACES

Theodore M. French

Inorganic Materials Research Division, Lawrence Berkeley Laboratory, and Department of Chemistry; University of California

Berkeley, California

ABSTRACT

Single crystal surfaces of electrical insulators, Al_2O_3, SiO_2, NaCl, NaF, and LiF have been studied by low energy electron diffraction. An ordered surface phase has been found on the (0001) face of aluminum oxide above 1250°C that has a unit mesh ($\sqrt{31} \times \sqrt{31}$) that is different from the unit mesh of the low temperature surface structure (1x1). Experimental evidence is presented to show that the order-order phase transformation [(Al_2O_3 (0001)(1x1) → rotated ($\sqrt{31} \times \sqrt{31}$)] is accompanied by a change in the chemical composition of the surface, i.e., the loss of oxygen. The structural change is reversible and either surface structure can be obtained alternately by heat treatment of the samples in oxygen (> 10^{-4} torr) or in the presence of excess aluminum on the surface.

The intensities and the positions of the diffraction peaks from the (100) crystal faces of LiF and NaF have been measured. It has been found that the single scattering (kinematic) model explains the observed positions of the diffraction beams. The intensities of the various diffraction beams of LiF and in NaF are compared.

The temperature dependence of the diffracted specular (00) beam has been measured for NaF(100). A surface Debye temperature of 90°K can be calculated from the measurements.

The rate of decomposition of the NaF crystal surface in the electron beam has been measured. The dependence of the rate of decomposition on temperature and on incident electron beam energy has been studied.

I. INTRODUCTION

Low energy electron diffraction is a uniquely powerful technique to study the structure of single crystal surfaces, the changes of surface structure as a function of chemical change, or changing temperature at the surface. Most of the low energy electron diffraction (LEED) studies so far have been carried out using metal or semiconductor single crystal surfaces. The purpose of the research which is described in this thesis is to carry out low energy electron diffraction studies on various insulator surfaces. These studies were to be carried out to verify and overcome the difficulties in obtaining surface structural information on insulating surfaces, to measure the intensities of diffraction beams back-reflected from single crystal surfaces of insulators, and to study the surface chemistry of insulating surfaces. These chemical studies involved monitoring the variation of surface structure with temperature and the interaction of the surface atoms and ions with the electron beam incident on the single crystal surface. For these studies we have selected the materials aluminum oxide (Al_2O_3), quartz (SiO_2), and alkali halides (LiF, NaF and NaCl).

The importance of carrying out investigations by low energy electron diffraction using insulator surfaces requires little justification. Most of the organic molecules and molecules of biological interest are insulators, and further surface studies using these molecules require prior solving of the experimental difficulties of electron scattering studies from insulating surfaces. Alkali halides are prototypes of ionic compounds, and solution of the difficulties

of low energy electron diffraction studies using these crystal surfaces would make an important contribution to surface structure analysis. Al_2O_3 and quartz are important materials in surface catalysis and therefore are likely candidates for surface structural studies.

First, I shall review the status of surface structure analysis using the low energy electron beams. Then the preparation of the various insulator surfaces will be discussed. Next, the experimental problems that are involved in carrying out the low energy electron diffraction experiments from electrical insulator surfaces are discussed. Then the experimental data is given as obtained from the structural and surface chemical studies for each of the insulators that has been investigated. Finally, the interaction of the electron beam with the various insulating surfaces is discussed.

II. THE DIFFRACTION OF LOW ENERGY ELECTRONS FROM SINGLE CRYSTAL SURFACES

A major obstacle of surface structural studies using low energy electron diffraction is the lack of a simple theory which can explain the scattered low energy electron beam intensities. The application of such a theory in model calculations where the only important variables are the atomic positions should lead, just like the use of kinematic theory and x-ray diffraction, to complete description of the surface structure. It is hoped that such a theory will become available in the very near future. Until then, the assignment of atomic positions of surface structures solely on the basis of the diffraction pattern is not unambiguous. This explains the different interpretations which may be given to the same diffraction pattern and the concentration of studies on only simple monatomic or diatomic surfaces. Frequently, however, the available supplementary chemical information using other experimental techniques permits one to identify the surface structure correctly and to eliminate most of the alternative models.

In order to carry out a LEED experiment one needs ultra high vacuum, one face of a pure single crystal and a well-focused electron beam in the energy range of 1-500 eV. At the present state of technology such an experiment can be carried out with relative ease. Many of the unique characteristics of LEED in the range of 1-500 eV are due to the large scattering cross-sections of low energy electrons. Particularly, at very low electron energies (1-100 eV) these cross-sections may be on the order of 1 $Å^2$. As a consequence, there will be substantial amplitude scattered into the non-forward directions and

the probability that the electron will be found in the transmitted beam will be significantly less than unity. This results in a high probability that an electron will be incapable of penetrating very deeply into the solid before it is scattered either elastically or inelastically out of the forward scattered beam. Therefore most of the intensity that is backscattered out of the crystal comes from either the surface or the neighborhood of the surface. This, of course, makes low energy electron diffraction an ideal tool for studying the structure of surfaces. Unfortunately, the very aspect that makes LEED valuable for surface structural analysis also complicates this analysis. This is because the scattering cross-sections are large; not only will the electron be scattered predominantly from the vicinity of the surface, but it will also have a significant probability of being scattered more than once. This phenomenon is multiple scattering, and at voltages where the cross section is high it vitiates the applicability of the kinematic theory of diffraction which has been used so successfully in the x-ray case where only single scattering or kinematic events are important.

One of the most important parameters which enters into all calculations of surface structure from the intensities of the diffracted low energy electron beams is the amplitude scattered by a single atom from the crystal surface. The amplitude in any given diffraction beam is dependent upon the probabilities that electrons will be scattered out of the primary beam or other diffraction beams, into that beam from various points in the crystal.

These scattering probabilities are dependent upon the atomic potential. Recent studies indicate that Hartree-Fock-Slater atomic

potentials can be used to obtain realistic scattering factors for low energy electron scattering. The atomic scattering process in the low energy range used in LEED experiments is complicated by the breakdown of the Born approximation. Atomic scattering factors must be obtained using atomic potentials by a phase shift analysis or from experimental differential cross-section measurements.

Another parameter which is important in calculating intensities of diffracted low energy electron beams from single crystal surfaces is the inelastic scattering of low energy electrons. The elastic mechanisms lead to the usual diffraction phenomena investigated by LEED. The inelastic mechanism must be extremely important in the interpretation of LEED information as inelastic processes are generally far more probable than elastic processes in the energy range where most LEED studies are performed. The inelastic scattering has the effect of attenuating most of the multiple scattering interactions between diffraction beams and of reducing the intensity of the back-diffracted electron beam. Recent studies by Duke and co-workers[1] have taken the inelastic damping of the scattered electron beam into account, and have aided the development of a realistic scattering model for surface structure calculations from the intensities of the back-diffracted low energy electron diffraction beams.

Another variable which enters into the low energy electron diffraction calculations is the surface Debye-Waller factor. Atoms in the surface are not rigidly held but are constantly undergoing thermal vibrations. The main effect of lattice vibrations is to scatter a fraction of the elastically back-scattered electrons out

of phase. Thus the intensity of the diffraction beam decreases, while the intensity of the background increases with increasing temperature. From studies of the temperature dependence of the intensity of the back-diffracted electron beam, the mean square displacement of surface atoms can be calculated. These calculations and experiments have been carried out for alkali halide crystals and will be described in a later section.

Finally, the inner potential is an additional variable in LEED calculations. When an incident electron strikes the crystal, due to the change in potential which it experiences, there is a corresponding change in the wavelength of the incident electron. This increase in the kinetic energy of the electron upon entering the solid is commonly described as being due to the inner potential. The electron is accelerated as it enters the solid since at interatomic distances the nuclei are only imperfectly shielded by the core and valence electrons. The average inner potential experienced by a primary electron will be dependent upon the energy of the electron as a degree of shielding of the positive nuclei will to some extent be dependent on the electron-electron correlation.

The usefulness of any theoretical analysis that is developed from various scattering models for low energy electrons depends on its reproducing the experimental results. Most of the experimental results are obtained by measuring the intensities of the back-diffracted electron beam as a function of electron energy. Thus such curves that are obtained experimentally, when available, should aid the development of theoretical analysis. For this

reason we have measured the intensities of back-diffracted electron beams as a function of electron energy from various alkali halide surfaces as well as from the (0001) face of α-alumina.

III. PREPARATION OF SINGLE CRYSTAL SAMPLES FOR LEED STUDIES

1. Alumina (Al_2O_3)

The Al_2O_3 crystals were the best grade available from the Union Carbide Corporation. A spectroscopic analysis showed the impurity levels in ppm: Mg, < 2 ppm; Si, < 4 ppm; Fe, < 2 ppm; Ca, < 2 ppm; Ga, < 2 ppm; Cu, < .5 ppm. Samples cut to size 5x7x1 mm, were supplied, already oriented to the (0001) face and polished. The crystals were chemically etched using potassium persulfate and boric acid mixed in equal parts by volume. The samples were heated in the etching mixture in an oven at 750°C in a gold-covered combustion boat for about 30 minutes. Weak diffraction beams were often observed without further treatment once the samples were placed in the ultra-high vacuum diffraction chamber. Another etch, concentrated phosphoric acid was also employed to prepare the surface of alumina. The crystal was immersed in phosphoric acid for 60 minutes at an oven temperature of 500°C. This treatment resulted in a badly pitted crystal. Nevertheless the diffraction pattern was visible from the pitted surface after it was heated to about 1100°C. This etching treatment was, however, abandoned in favor of chemical etching using the potassium persulfate-boric acid mixture.

Crystal mounting and heat treatment. The alumina crystal sample was mounted in a star-shaped piece of 1 mil tungsten foil. The points of the star were bent around the sample to hold it securely. There was minimum contact of the points with the front surface. The tungsten foil was spot-welded to tantalum supports which were attached to the crystal holder and manipulator. The crystal was

heated by conduction from the resistively heated tungsten foil. The temperature was measured by an optical pyrometer focused on a tungsten film which had been vacuum evaporated on a small area in the back of the sample. The error in measuring the sample temperature is difficult to estimate but should be less than ±100°C. Vacuum evaporation by heating the crystal to high temperatures (~ 1500°C) was used most frequently to clean the alumina surface. Ion bombardment could also be used for surface cleaning. Ion bombardment using 1-2 keV Ar ions disordered the alumina surface and eliminated the diffraction features. Heating above about 900°C after ion bombardment would restore the surface order. The minimum conditions of ion bombardment to disorder the diffraction pattern were 10^{-5} torr argon, 2 keV accelerating potential, and 4 milliamp ionizing electron flux, ~ 4×10^{-6} ion current for 10 minutes.

2. Alkali Halides

A surface preparation of LiF, NaF, and NaCl samples was much easier than that of alumina surfaces. These alkali halide single crystals were purchased from Harshaw Chemical Corporation. They were cleaved by a razor blade to a size of 5x7x1 mm discs, were etched in absolute methanol and were placed into the diffraction chamber using a platinum holder with similar geometry to that used for mounting the aluminum oxide samples. We attempted to clean the alkali halides by ion bombardment and subsequent heating. Even long ion bombardment at pressures of 4×10^{-5} torr of xenon for 6 hours on sodium fluoride using 135 eV ions, neither removed the pattern nor improved it.

It appears that ion bombardment introduces non-stoichiometry at the surface but there is no permanent surface damage due to the rapid annealing by vacancy diffusion of the surface structure.

High temperature heating of these samples was used to clean the surfaces by vaporization of the topmost layers of the alkali halide crystal samples. The temperature of the heat treatment was 800°C for LiF, 850°C for NaF, and 400°C for NaCl for 15 minutes. Then the alkali halide was annealed for an additional hour at a temperature about 200° lower. Since the alkali halide surfaces interact with the incident electron beam the annealing for one hour at a lower temperature was also used to regenerate the crystal surface to its original less-damaged state after the electron diffraction study. However the accumulated damage due to electron bombardment of the crystal surface for a long time was so great that a longer annealing period was necessary at the same temperature.

3. Silicon Dioxide (Quartz)

The SiO_2 crystal was cut from a large crystal by means of a diamond saw. The damage from sawing was removed by polishing down to 1 micron diamond grit using an impregnated aluminum wheel. The crystal was etched using boiling concentrated aqueous HF in a Teflon beaker. A long period of time is necessary to produce significant etching. On the c face 1 hour of boiling was enough to get a diffraction pattern. Eight hours of boiling removed about 2 mils of material from each face. Short heating (15 minutes) at about 1000°C was all the additional treatment necessary to get the diffraction pattern.

IV. ELIMINATION OF SURFACE CHARGE AT INSULATOR SURFACES DURING LEED STUDIES

When electrons in the range 5-100 eV strike the aluminum oxide or alkali halide surfaces, a surface charge builds up rapidly so as to repel the incident electron flux before it can penetrate the crystal or be scattered by the periodic atomic potential at the surface. Thus, under usual operating conditions that are employed in LEED studies of metal surfaces, no diffraction pattern can be obtained from either aluminum oxide or alkali halide surfaces below a certain voltage, usually 50-100 eV. This negative surface charge build-up poses serious limitation to structural studies of insulator surfaces since most of the experimental information about the surface structure is obtained in the electron energy range 30-120 eV. Above these energies a larger fraction of the electrons penetrates below the surface and the backscattered beam contains more information about the bulk than about the topmost atomic layer. Therefore in LEED studies of insulator surfaces it is imperative that this negative surface charge layer be removed from the studied surface.

There are several methods for removing the negative space charge build-up on insulators in LEED experiments. These involve either conducting the surface charge away or using the secondary electron emission properties of the crystal to disperse the incident electron flux by allowing it to be re-emitted. We have been successful in removing the negative surface charge layer from the (0001) face of alumina by the simultaneous application of two electron guns. One, operating at 1-2 keV at a grazing angle of incidence 15°, was

continuously discharging the surface, while the usual LEED gun, operating in the range 10-350 eV, was used to obtain the diffraction pattern. This technique should be applicable for the elimination of negative surface charge from all those insulator surfaces which, a) have a secondary electron emission flux above a given incident electron energy which is larger than the incident electron flux, and b) do not decompose or otherwise interact chemically with the high energy electron beam. It is well known that for many insulators the yield of secondary electrons which leave the solid during electron bombardment is greater than the incident electron flux above a certain threshold energy of the incident electron beam. The incident electron energy at which the ratio of the secondary electron emission current and the incident electron beam current becomes larger than unity, is often called the secondary emission cross-over. By continuously spraying the insulator surface with electrons with energies above the secondary cross-over the surface can be discharged or a small positive surface charge may be established. Since this positive surface charge attracts electrons toward the crystal it does not affect the diffraction process, although it may change the energy of the incident electrons to a small extent. The secondary emission cross-over for the clean (0001) face of alumina which exhibits a (1x1) surface structure appears to be in the range 80-100 eV. The cross-over energy varied within this range from sample to sample and was found to be dependent on the purity of the surface. Slight contamination, as detected by x-ray fluorescence, of the sample by tantalum which was often used at first as a crystal holder, could increase the cross-over to over 200 eV. The secondary

emission cross-over may also depend on the chemical surface composition. When the surface structure was changed to an ordered oxygen-deficient surface structure (to be discussed later) the cross-over energy decreased to approximately 50 eV. Since heat treatment was necessary to produce this new structure and the accompanying changes in surface composition, the possibility of unwanted impurities diffusing to the surface and aiding the reduction of the cross-over cannot be eliminated. It is likely, however, that the lowering of the secondary emission cross-over is caused by the change in the surface composition of the (0001) face of alumina.

Since the electrons from the high energy electron gun which is used to eliminate the negative surface charge are energetic enough to pass through the grid system of the electron optics and reach the fluorescence screen, the background intensities increased. This, however, does not prevent the detection of diffraction spots from fairly ordered alumina surfaces to as low as 25 eV incident electron beam energy from the LEED electron gun. The high energy electron flux which is used to discharge the surface was cut back to a minimum in order to minimize the background intensity on the fluorescence screen. Figure 1 gives the secondary emission cross-over for the α-alumina with a (1x1) surface structure as a function of the ratio of the current from the high-energy electron gun, i_2, and the LEED electron gun, i_{LEED}, for two different electron energies of the discharging gun. The cross-over decreases with increasing i_2/i_{LEED} ratio at first, but above $i_2/i_{LEED} = 2$ the ratio remains constant. The cross-over appears to be independent of the discharging gun energy in the range 1000-2000 eV. No studies have been made with

the discharging gun below this energy range. Although our technique, i.e., the simultaneous use of two electron guns, is successful in removing the space charge, other techniques (vide infra) might also be employed in studies of insulator surfaces to remove the unwanted surface charge.

For alkali halide crystals NaF, LiF, and NaCl samples that were used in this study, LEED studies can be carried out at elevated temperatures using thin samples in order to increase the ionic conductivity sufficiently. Also the secondary emission from the NaF crystals was sufficient, for the experimental range of electron energies, to remove the surface space charge as soon as the sample was placed in the diffraction chamber. For the alkali halide samples the secondary emission was sufficient to discharge the surfaces until the crystal had been in the electron beam for 20 minutes. After 20 minutes the secondary emission crossover energy rises sufficiently to distrub measurement of the diffraction beam intensities. As will be discussed later, electron beam impact dissociates the surface of alkali halides and such a result is very likely to be due to changes in surface chemical composition of these alkali halide single crystal samples.

V. THE LOW ENERGY ELECTRON DIFFRACTION EXPERIMENT

In the LEED experiments the electrons are obtained by thermionic emission from a hot cathode. In these studies the cathode had an operating surface temperature of ~800°C. The energy spread of the emitted electrons at this temperature is of the order of .2 eV. These electrons are then focused electrostatically and allowed to impinge on the crystal surface which is held at ground potential. The electron beam is on the order of 1 mm in diameter. For a completely ordered surface the coherence length of the electron to a large extent is determined by the size of the source of the electron beam. The incoherence within the electron wave packet sets an upper limit to the number of atoms which can contribute to coherent scattering. The coherence width of the electron beam in a typical low energy diffraction apparatus is about 500 Å. Thus, no area larger than 500 $Å^2$ can contribute coherently to the diffraction patterns since no area larger than this received coherent radiation. The question of the minimal area necessary to give a coherent diffraction pattern has not been definitely answered experimentally. However if one assumes that ordered areas of 25-100 atoms are sufficient to give coherent diffraction best agreement with present results is obtained. LEED experiments indicate that the number of elastically scattered electrons which are back-reflected from crystal surfaces varies with the incident electron beam energy markedly. About 20% of the incident electrons are back-scattered elastically at 10 eV and about 1% at 100 eV and less at higher energies. The scheme of the electron optics is shown in Figure 2. The backscattered electrons

travel a field free path to the first grid which is also held at ground potential,as is the crystal. Energy analysis takes place at the second grid which is held at cathode potential. This grid in principle repels all of the electrons which have lost energy in collision with the surface and allows only the elastically scattered electrons to penetrate through. The elastic component which has penetrated the grid system is then accelerated by the application of a large positive potential (5000-7000 eV) onto the fluorescence screen where, due to the radiative recombinations after excitation by the electron beam, light is emitted where the electron beam hits. The light intensity is proportional to the number of electrons hitting the screen. This post-acceleration technique is an excellent means of instantaneously displaying the diffraction pattern. The solid angle subtended by the fluorescent screen is 95°.

There are other detection techniques which are often used in LEED studies. A Faraday cup which can be rotated 180° is frequently used to monitor the low energy electron beam intensity. While the fluorescence screen techniques allow one to measure relative intensities the Faraday cup detection allows absolute intensity measurements which are necessary for some experiments.

The fluorescent screen can be readily photographed and one obtains a photographic display of the diffraction pattern which can also be used to analyze the intensities of the different diffraction spots using densitometers of different types.

VI. INTENSITY DATA

The most easily obtainable diffraction beam that can be studied by LEED is that of the specularly reflected (00) beam. Usually in LEED experiments the intensity of the diffraction beams is monitored as a function of electron beam energy. The intensity of the (00) spot may be obtained without moving the measuring device (spotphotometer, for example) since the scattering vector for that particular reflection is always perpendicular to the surface plane. Thus, the angle at which the (00) diffraction spot appears does not change with variation of the electron energy. Unfortunately, moving of the (00) spot caused by space charge that builds up at the insulator surface negates all these advantages. The diffraction spot may wander because of stray electrostatic or magnetic fields. One can compensate for this by using a wide enough aperture on the spot-photometer that was used to measure the intensity of the (00) spot as a function of beam voltage. In this study the aperture of the spotphotometer was about 20 minutes at approximately 2 meter distance and a balancing magnet to block out external magnetic fields was also used.

The zero drift, i.e., change of apparent electron energy during the measurement which is due to the build-up of the surface charge, was especially serious for Al_2O_3. For alkali halides the voltage measurements were reproducible within ±5 volts except at very low beam voltages (below 70 v). The state of order at the surface can also affect the intensities of the diffraction beams. As the crystal becomes more and more disordered the intensities of the diffraction

beams change at the different energies. Such a surface dissociation effect made measurements of the intensities from alkali halide surfaces very difficult to carry out. In order to alleviate this problem the decomposition rate of the alkali halide surfaces in the electron beam was studied separately and will be discussed in a later chapter.

In order to avoid the difficulties of surface decomposition during electron scattering from alkali-halide surfaces, a rapid beam voltage scan technique for surface intensity measurements was developed. The intensity vs. beam voltage plot for alkali halide surfaces using the (00) beam was made by using a 300-volt/amp generator which allowed to sweep the beam voltages within a second from 0-300 volts and this way the I_{00} vs. eV curves on alkali halide surfaces could be obtained during times much shorter than the times necessary to change the intensities detectably due to the decomposition rate of the surfaces at room temperature. The I_{00} plots as a function of electron energy for alkali halides showed a fairly good consistency. The surface could always be annealed before or after the measurements by repeated vaporization of the surface, which improved the surface stoichiometry. The intensity vs. beam voltage curve for two alkali halide surfaces, NaF and LiF using the (00) diffraction beams are given in Figure 3. Table 1 shows the observed position of the different diffraction beams. Also Fig. 4 shows the observed positions of the beams against the predicted positions.

There are three variables that should define the diffraction beam properties: the angle of scattering with respect to the surface normal, θ; the incident energy; and the intensity. The intensities of the various diffraction beams from NaF and LiF single crystal (100)

surfaces are plotted on a three dimensional plot which displays the intensities, the angle of scattering and energy, in Figures 5 and 6. There are two types of diffraction beams distinguishable, those which are characterized by odd values of Miller indices, and those which are characterized by even values of the Miller indices. Since for the alkali-halide compounds there are two ions per unit cell, the intensities of the even spots are proportional to the square of the sum of the scattering factors of each type of ion. The intensities of the odd Miller index diffraction beams are proportional to the square of the difference of the scattering factors, assuming a single scattering model. Based on this model the ratio of the intensities of I_{odd}/I_{even} can be written as

$$\begin{matrix} I_{odd} \propto (f_1-f_2)^2 \\ I_{even} \propto (f_1+f_2)^2 \end{matrix} \quad ; \quad r \equiv f_2/f_1 \quad ; \quad I_{odd}/I_{even} = \frac{(1-r)^2}{(1+r)^2}$$

It can be seen from Figures 5 and 6 that the diffraction beams characterized by odd Miller indices have much lower intensities than the diffraction beams that are characterized by even Miller indices, as expected from the single scattering model.

The intensity of the (00) diffraction beam as a function of electron energy under conditions of near normal incidence are also plotted for the (0001) face of Al_2O_3, and this is shown in Figure 7.

Of course the diffraction experiment gives one no information about which of the two scattering centers scatters the more strongly. There is, however, a simple analogy which will allow a guess at this. The scattering factors of Na^+ and F^- are approximately the same.

This follows from the data since the odd spots are so weak as to be almost invisible. One might therefore conclude that isoelectronic ions have approximately the same electron cross section, at least in the regions covered by the experiment. By analogy with the x-ray case then -- since the above is also true for the x-ray case--one might expect the scattering to be related to or even proportional to the number of electrons for x-rays or to the depth of the potential well for electrons. One would therefore expect that the scattering from the small Li^+ ion would be much less than the scattering from the F^- ion. It is more difficult to determine whether Na^+ or F^- is the strongest scattering center -- it is pleasing to assume that the valence electrons are the same (roughly) in both these ions and that the scattering is dominated by the contribution of the potential wells. The Na^+ would scatter more if this tenuous assumption were true since it has a higher nuclear charge and a deeper potential well. The numerical value ratio of the scattering factors as a function of eV and angle may be estimated from the interpolated values of odd and even intensities.

VII. TEMPERATURE DEPENDENCE OF DIFFRACTION BEAM INTENSITIES

It is of importance to measure the temperature dependence of the diffraction beam intensities back-scattered from the single crystal surfaces since thesedata could be used to calculate the mean square displacement of atoms in the surface or the surface Debye temperature of the material that is being studied. Several problems arise in measuring the temperature dependence of insulators that do not arise in the same experiments on metal surfaces. The temperature of the alkali halide crystal must be measured by means of a thermocouple that is sandwiched between the slides of the same material. This is necessary because with insulators spot welding or other methods of securely attaching the thermocouple to the studied crystal are not usually feasible. Attaching the thermocouple to the crystal holder would result in an erroneous temperature measurement since the holder, in general, is not in good thermal contact with the single crystal. The rate of cooling of metal crystals could be fast, due to the excellent heat conduction through the holder. The rate of cooling of insulator crystals in our experiments was slow, taking about 10 minutes or more to approach 300°K from 600 or 800°K since the crystal was not in good thermal contact with the holder. Charging of the crystal surface, of course, would also make the monitoring of the intensities of the diffraction beams difficult to carry out. In addition, the possibility of the chemical decomposition of the surface under electron beam incidence cannot be overlooked. We were able to carry out the temperature dependence measurements of the diffraction beam intensities under slow cooling

conditions using a special technique. The beam of electrons was deflected from the crystal except for short periods of time when the measurements were made.

The intensity of scattered electrons, neglecting multiple scattering events, is given by

$$I_{hk\ell} = |F_{hk\ell}|^2 \exp[-(16\ \pi^2 \cos^2\phi/\lambda^2) < u^2 >] \qquad (1)$$

where the exponential term is the Debye-Waller factor, λ is the electron wavelength, ϕ is the angle of incidence with respect to the surface normal, and $|F_{hk\ell}|^2$ is the scattered intensity by the rigid lattice. Using the Debye model of lattice vibrations in the high temperature limit, the mean square displacement is given by

$$< u^2 > = (3Nh^2/Mk)[T/(\theta\infty)^2] \qquad (2)$$

where $\theta\infty$ is the Debye temperature at the high temperature limit, M and T are the atomic weight and the temperature of the solid, respectively, N is Avogadro's number and k and h are the Boltzmann and Planck constants. Combining these two equations we have

$$I_{hk\ell} = |F_{hk\ell}|^2 \exp\left\{-(12Nh^2/Mk)(\cos\phi/2)^2[T/(\theta\infty)^2]\right\} \qquad (3)$$

The logarithm of the intensity of the (00) diffraction beam plotted as a function of temperature T gives a straight line. From the slope, the root mean square displacement in the direction perpendicular to the surface plane, $u_\perp$ can be calculated. Of course, this can only be obtained if the (00) diffraction beam is used to monitor the temperature dependence of the intensity of back-scattered electrons. In order to obtain the Debye-Waller factor from the experimental

intensity curve, the background intensity has to be subtracted. This way the contribution of thermal diffuse scattering to the total intensity is removed. We have found that for alkali-halide crystals, just as in the case for metal surfaces, the measured values of the Debye temperatures were strongly dependent on the electron beam energy. It is apparent that with increasing electron energy a larger fraction of electrons scatter from atomic planes which lie below the surface plane. Thus, at higher electron energies the experimentally determined Debye temperature approaches the bulk Debye temperature value. The Debye temperature which is characteristic of the surface atoms can be obtained from data taken using a very low energy electron beam. At such low energies the largest fraction of the impinging electrons backscatter from the surface atoms without penetrating deeply into the crystal lattice. The effective Debye temperature calculated from the log I vs. T curves, using Eq. 3, is plotted as a function of beam voltage for the (100) face of NaF. This is shown in Figure 8. It is apparent that the surface Debye temperature is much smaller than that of the bulk value. The surface Debye temperature for NaF is about 90°K, a value that is about .22 times the bulk value ($\theta_{bulk} \simeq 410°K$).

It would have been useful to measure the surface Debye temperature at electron energies nearer to zero electron energy. This was not possible in our experiment due to the charging of the crystal. Thus the lowest electron energy at which measurements could reliably be made was 50 eV.

The typical value for the surface Debye temperature on f.c.c. metals is about .5 times that of the bulk value. Values for the ratio

of the surface Debye temperature to the bulk Debye temperature, for various materials is given in Table 2. This ratio appears to be significantly smaller for NaF than for the studied f.c.c. metal surfaces. It appears that the differences in the chemical properties of these two types of compounds should be responsible for the large differences in the observed surface-to-bulk Debye temperature ratio.

VIII. THE DECOMPOSITION OF ALKALI-HALIDE CRYSTAL SURFACES IN THE ELECTRON BEAM

We have observed that the intensities of diffraction beams back-scattered from NaF, LiF and NaCl surfaces have decreased as a function of time at 300°K. Similar observations were made by Gallon, et al.,[2] and by Palmberg and Rhodin,[3] indicating that the deterioration of the pattern is due to the interaction between the surface ions and the electron beam. These same writers have also observed the evolution of halogen gas atoms and molecules from the alkali-halide crystal surfaces during electron bombardment using a mass spectrometer. Since our purpose was to measure the intensity vs. eV curve for several diffraction beams accurately for the alkali-halide surfaces, we have to determine the effect of the electron beam on the structure of the crystal surface. For this reason we undertook a study of the kinetics of the surface decomposition of NaF by low energy electrons. A constant electron flux about 10^{-3} amp cm^2 was incident near normal on the crystal surface at a given temperature T in the range 300-450°K and at a given energy. The intensity of the specular (00) beam was measured as a function of time t. Sets of I vs. t curves at different temperatures were taken at different electron energies in the range 90-225 eV. The decrease of the diffraction beam intensity is due to the removal of the surface ions from the ordered domain that are responsible for the diffraction. This is by some disordering process or by decomposition of the surface structure due to a chemical surface reaction that takes place upon the interaction of the electron beam and the surface

ions. Since independent evidence[2,3] indicates that the surface decomposes readily upon electron impact, we shall assume that chemical decomposition is the dominant process. Let N be the concentration of ordered surface sites in units of cm^{-2}. Since the intensity of the back-diffracted electron beam, I, is proportional to the concentration of ordered ions on the surface, i.e., $I = kN$, the rate of decomposition was taken to be proportional to the intensity change as a function of time.

We have found that increasing the temperature causes a decrease in the decomposition rates under electron impact. A typical set of curves taken at different temperatures is shown in Figure 9. Changing the energy of the incident electron beam seems to have little effect, within experimental accuracy, on the decomposition rate except at the highest voltages used (see Figure 10). The rate of decomposition increased with voltage, but only to a significant extent at about 225 eV, the highest electron energy at which the decomposition rates were studied. Since increases in the surface temperature decrease the rate of decomposition as measured by the time dependent decrease of the diffraction beam intensity, it appears that surface damage that is created by the impinging electron beam is being removed by annealing, i.e., temperature induced diffusion or annihilation of defects that were created by the electron beam at the surface. In fact, we were able to eliminate the time dependent deterioration of the diffraction beam intensities altogether by heating the crystal to a high enough temperature so that the defect removal rate equaled the decomposition rate. This occurred at about 450°K for NaF.

Let us now analyze the kinetics of decomposition assuming the following model for the decomposition. This model gives good qualitative fit to the experimental data and allows the evaluation of the activation energy for the process that removes the damage. Some assumptions have been made in this model. 1) The damage due to interaction of the surface ion with the electron beam that decreases the diffraction beam intensity decreases exponentially with distance from the surface of the crystal. Let the form be given by $e^{-\alpha x}$, α having units of cm^{-1}. This is likely because the intensity of the electron beam dies off exponentially from the surface.[4] 2) The process for removing the damage from the surface can be assumed to be ion or vacancy diffusion. In steady state it should obey Fick's first law, $J(x) = -D_T\, dp/dx$, where J is the flux of diffusible materials, ions or vacancies, in units of sites/cm^2 sec, D_T is the diffusivity in units of cm^2/sec, and p is the concentration of the damaged sites in units of sites/cm^3.

Under the experimental conditions the crystal starts out with some initial damage density in it. This initial surface condition of the crystal was reproduced for each run as nearly as possible. Let us say that the initial damage density at the surface is p_o (in sites/cm^3). Then, $p(x) = p_o e^{-\alpha x}$ using assumption (1). Using Fick's law, $J(x) = \alpha D_T p_o e^{-\alpha x}$, and at the surface, $J(0) = \alpha D_T p_o$. The escaping damage flux at the surface is the rate of annealing. If N_o is the total number of ordered sites/cm^2 in the absence of damage then N_o-N is the total number of damaged sites/cm^2. The total amount of damage in the crystal per unit area is the damage density times unit area integrated from the surface into the crystal. Hence:

$$N_o - N = \int_0^\infty p(x)dx \ , \tag{5}$$

$$N_o - N = p_o/\alpha \tag{6}$$

$$p_o = \alpha(N_o - N) \tag{7}$$

The observed rate of change in the crystal is equal to the damage done by the beam less the rate of annealing. The rate at which damage is done is proportional to the concentration of undamaged surface sites N and to the incident electron current i_{cur}. The rate of annealing is equal to the flux of damaged sites escaping at the surface. Thus,

$$dN/dt = -k_2 i_{cur} N + J(0) \tag{8}$$

$$dN/dt = -k_2 i_{cur} N + \alpha D_T p_o \tag{9}$$

$$dN/dt = -k_2 i_{cur} N + \alpha^2 D_T (N_o - N) \tag{10}$$

$$dN/dt = -k_2 i_{cur} N - a^2 D_T N + \alpha^2 D_T N_o \ . \tag{11}$$

All these quantities have units of flux.

The experimental points in Figure 12 which showsthe rate of decomposition vs. temperature, were obtained from intensity vs. time data. The intensity vs. time data of Figure 9 were replotted on semi-log paper in Figure 11. The slopes of the resulting curves were obtained with a strong bias given toward the first few points. This was done since the first points have the best signal-to-noise ratio and because the method of initial slopes is used in their interpretation.

The slopes of the curves in Figure 11 give the rate constant for decomposition. These slopes were then replotted in Figure 12, with one point in Figure 12 for each line in a plot of the type shown in

Figure 11. Each plotted slope was normalized by dividing by the initial intensity.

If all the runs were started at the same initial concentration of damage $(N_o - N')$ then we have:

$$(dN/dt)_{N=N'} = -k_2 i_{cur} N' + \alpha^2 D_T (N_o - N') \qquad (12)$$

Every attempt was made to make sure the initial condition was the same from run to run; deviations from the same initial condition account for the spread in the data. Dividing by the initial concentration of damage N':

$$\frac{1}{N'}(dN/dt)_{N=N'} = -k_2 i_{cur} + \alpha^2 D_T (N_o - N')/N' \qquad (13)$$

Since the measured experimental quantity, the slope in Figure 11, is $\frac{1}{I'}(dI'/dt)$, we apply the equation $I = kN$ to get:

$$\frac{1}{I'}(dI/dt)_{I=I'} = -k_2 i_{cur} + \alpha^2 D_T (I_o - I')/I' \qquad (14)$$

Hence the observed normalized rate of decomposition is $\left\{\alpha^2 D_T (I_o - I')/I'\right\} - k_2 i_{cur}$; this quantity is the real rate of decomposition plus $k_2 i_{cur}$ subtracted from the rate for annealing, $\alpha^2 D_T (I_o - I')/I'$.

At 300°K the decrease of intensity of the diffraction beams is rapid. At this temperature the rate of annealing (the second term of the right hand side of Eq. 14) must be at least an order of magnitude smaller than the actual rate of decomposition (the first term on the right side of Eq. 14). As long as there is a sufficient number of ordered surface sites N, the decomposition can be considered constant (temperature independent) since the electronic excitation that leads to decomposition may take place at any temperature. This is

clearly shown by the experimental data in Figure 12. Thus we obtain the rate of annealing that is strongly temperature dependent by subtracting the constant rate of decomposition, $k_2 i_{cur}$, from the observed rate. This is accomplished when the data in Figure 12 is replotted in Figure 13. From every point of the curve fitted to the experimental points is subtracted the quantity .05 sec^{-1} which corresponds to the real rate for decomposition, $k_2 i_{cur}$.

The temperature dependence of the rate of annealing is of the form $A(T) = A_o e^{-E/RT}$. To obtain the activation energy of the annealing process the fitted curve of Figure 12 is replotted in Figure 13 as log A(T) vs. 1/T. The slope of this line is the quantity 1/2.30(E/R). A value for E of about 7.8 kcal is obtained from this plot.

Values for fluoride ion diffusion are not easily obtained due to the lack of readily available fluorine tracer nuclei. It is probabl , however, that the values of fluorine diffusion and fluoride ion vacancy diffusion are near the values of that for chloride ion diffusion in NaCl. These values are 53 kcal for Cl ion diffusion in NaCl,[5] and 20 kcal for chloride ion vacancy diffusion in NaCl.[6] The value 7.8 kcal would be very low for fluoride ion diffusion, we believe. It is, however, in the right range for surface vacancy diffusion since the surface diffusion of the species that are also diffusing in the bulk that have face centered cubic crystal structures have in general activation energies roughly $\frac{1}{2}$ that of the bulk diffusion activation energies. This is due to the change of mechanism of surface diffusion with respect to bulk diffusion due to the lower number of neighboring ions at the surface that lower the binding energy of the diffusing species at a given surface site.

IX. SURFACE CHEMISTRY OF ALUMINA

The structure of alumina is different from that which is expected by the projection of the bulk unit cell to the various crystal surfaces. The (0001) crystal face exhibits its (1x1) bulk-like structure up to 1250°C under vacuum. It rearranges, however, above this temperature to give a weak $(\sqrt{3}x\sqrt{3})$ rotated 30° surface structure. Upon further heating at the same temperature, the $(\sqrt{31}x\sqrt{31})R\pm9°$ surface structure, which is stable to the highest studied temperature of 1700° is formed. Schematic representations of the resultant diffraction patterns are shown in Figure 11. It is customary to designate the complex surface structures by the coefficients of the transformation matrix which generates the structures with the two unit cell vectors of the bulk-like substrate, vectors of equal length, 4.76 Å and 60° apart. This is given for the rotated $(\sqrt{31}x\sqrt{31})$ pattern by

$$A = \begin{pmatrix} 11/2 & \sqrt{3}/2 \\ -\sqrt{3}/2 & 11/2 \end{pmatrix} \qquad B = \begin{pmatrix} 11/2 & -\sqrt{3}/2 \\ \sqrt{3}/2 & 11/2 \end{pmatrix}$$

These matrices generate the basis vectors for two domains, A and B, which must be present on the surface simultaneously in order to generate the opposite diffraction pattern. This diffraction pattern is shown in Fig. 15 . These domains are formed from the

original unit mesh be expanding the unit vectors by a factor of $\sqrt{31}$ and by rotating them ±9°. We shall show evidence that the alumina surface which exhibits the rotated ($\sqrt{31}$x$\sqrt{31}$) surface structure is oxygen deficient. The other two crystal faces which have been studied, the ($\bar{1}012$) and the ($11\bar{2}3$) orientations, have (2x1) and (4x5) surface structures, respectively, at high temperatures (> 900°C). We have been able to confirm the presence of the surface structures on the (0001) face of α-alumina, which have also been reported by Charig[9,12] and Chang.[7,8] Due to the reproducibility of these surface characteristics there can be little doubt that these structures are the property of the clean alumina. We have not employed electron bombardment heating on the samples in our experiments to avoid difficulties in interpreting our results, which are due to the well-documented interaction of the high energy electron beam with the crystal surface.

Properties of the rotated ($\sqrt{31}$x$\sqrt{31}$) surface structure. Heating by radiation the freshly etched (0001) alumina surface which exhibits the (1x1) surface structure under vacuum above 1250°C readily produces the rotated ($\sqrt{31}$x$\sqrt{31}$) surface structure. During its formation, oxygen evolution is detectable by mass spectrometry. Oxygen evolution was also detected by Charig[9] during the formation of the rotated ($\sqrt{31}$x$\sqrt{31}$) surface structure by electron bombardment heating above 900°C. Ion bombardment using high energy (2 keV) Ar ions disorders the surface structure. The ($\sqrt{31}$x$\sqrt{31}$) surface structure is readily regenerated, however, by annealing the surface at approximately 800°C. Ion bombardment appears to disorder the surface without changing the ratio of aluminum to oxygen in the

topmost layers. Thus, once it forms upon heat treatment at high temperatures, the surface structure is extremely stable and reproducible under various experimental conditions. Its stability temperature range is clearly shown by the silicon deposition studies which have been made to investigate the epitaxy of silicon on the (0001) alumina surface. Silicon is known to etch the alumina surface by removing both aluminum and oxygen acccording to the overall reaction $3Si(g) + Al_2O_3 = 3SiO(g) + 2Al(g)$. Chang has detected all of the gaseous species in their proper atomic ratios by mass spectrometry.[8] Charig, by heating the alumina surface above 1000° after deposition of silicon at lower temperatures, either on the (1x1) or on the rotated ($\sqrt{31}$x$\sqrt{31}$) surface of alumina has regenerated the rotated ($\sqrt{31}$ x$\sqrt{31}$) surface structure.[9] Heating the (0001) face below 900°C after silicon deposition yields (1x1) bulk-like surface structure.

In order to establish that the stable high temperature rotated ($\sqrt{31}$x$\sqrt{31}$) surface structure has a chemical composition which is different from that of the low temperature (1x1) surface structure and to establish its stoichiometry we have heated the (0001) face in excess oxygen and aluminum vapor. When the rotated ($\sqrt{31}$x$\sqrt{31}$) surface structure is heated in oxygen at pressures larger than 10^{-4} torr, (these pressures considered to be high in ultra high vacuum LEED studies) at 1200°C the (1x1) surface structure was obtained. Removal of the oxygen and heating to a slightly higher temperature (1250°C or higher) under vacuum caused the reappearance of the rotated ($\sqrt{31}$x$\sqrt{31}$) surface structure. This reversible phase transformation could be induced at will upon introduction or removal

of oxygen. The reproducible reversible behavior of the transformation makes contamination, for example by WO, where the interaction with tungsten is due to the fact that tungsten is the sample holder material, unlikely as a mechanism for the transformation. Pressures lower than 10^{-4} torr of oxygen did not induce detectable changes in the high temperature surface structure during the usual heat treatment time (15 minutes). When aluminum metal was condensed on the (0001) alumina surface which exhibits the (1x1) surface structure, the rotated ($\sqrt{31} \times \sqrt{31}$) surface structure was formed by heating to about 800°C. In the absence of excess aluminum on the surface, the (1x1) surface structure would have formed at this temperature.

The fact that in oxygen the (1x1) structure is regenerated in the temperature range of 1200°C where the rotated ($\sqrt{31} \times \sqrt{31}$) structure is stable and with aluminum the rotated ($\sqrt{31} \times \sqrt{31}$) structure is formed in the temperature range 800°C where the (1x1) structure is stable, indicates that the (0001) face of alumina undergoes a surface phase transformation from a (1x1) surface structure to an oxygen-deficient rotated ($\sqrt{31} \times \sqrt{31}$) surface structure which is stable at high temperatures. This phase transformation can be made reversible by variation of the chemical surface composition using excess oxygen or aluminum. The transformations which have been found to occur under the various experimental conditions are summarized in Fig. 16.

The following statements summarize the results of our experiments, which can be used to interpret these surface structures of the (0001) face of α-alumina.

1) Upon heating the (0001) face of alumina which exhibits a (1x1) surface structure, in vacuum at temperatures larger than 800°C, a new ordered surface structure which can be characterized as ($\sqrt{3}$ x$\sqrt{3}$) rotated 30° appears. Subsequent heating to even higher temperatures produces the ordered rotated ($\sqrt{31}$ x$\sqrt{31}$) surface structure. Simultaneously, there is oxygen evolution from the surface. This surface structure, once formed, is extremely stable under a variety of experimental conditions.

2) Heating the high temperature rotated ($\sqrt{31}$ x$\sqrt{31}$) surface structure in oxygen at pressures > 10^{-4} torr at 1000-1200°C restores the low temperature (1x1) surface structure. Excess aluminum on the (0001) surface, on the other hand, catalyzes the reverse order-order transformation. These results would indicate that the ordered surface structures which appear at high temperatures are oxygen deficient with respect to the bulk structure of alumina. The transient ($\sqrt{3}$ x$\sqrt{3}$) surface structure can be explained to form by removal of oxygen atoms or by the addition of aluminum atoms to the (0001) surface. A possible model of the rearranged surface which would give rise to the observed diffraction pattern is shown in Figure 17. Other explanations are also possible. In all of the proposed models, however, the substrate serves as a template for the arrangement of the surface atoms.

Many of the diffraction patterns which exhibit fractional order diffraction beams can be rationalized in a straightforward manner. The extra spots appear at positions which are some fraction of the distance between the integral ordered diffraction beams and they indicate the appearance of the new surface periodicity which is an

integral multiple of, and is parallel to, the bulk unit cell. Such a surface structure can be generated by periodic buckling of the surface or as a result of partial occupation of the available surface sites. The surface structure thus formed retains the symmetry of the underlying substrate and there is little reason to postulate any marked change in the chemical bonding of the surface atoms with respect to the atoms in the bulk. It is however difficult to explain the appearance of large surface unit cells which are also rotated with respect to the bulk unit cell without invoking significant chemical rearrangement of the surface layer. The rotated $(\sqrt{31} \times \sqrt{31})$ unit mesh signifies mismatch between the newly formed surface structure and the underlying hexagonal substrate. The surface atoms which are built into the new structure can no longer adjust to the symmetry of the substrate and the observed diffraction pattern is likely to be due to the coincidence of lattice sites between the rearranged surface layer and the hexagonal substrate.

Let us assume that along with the change in chemical composition the aluminum cation, Al^{3+} is reduced in the oxygen deficient surface layer to the Al^{+} or Al^{2+} oxygen state. The ionic radius would be expected to increase as the valency is decreased. Let us estimate the ionic radius of Al^{+} ion. This ion may be more stable than the Al^{2+} ion because it has a pair of s electrons in the outer shell. It can be assumed that the radii of isoelectronic atoms and ions are inversely proportional to the effective nuclear charges.[10] Using this rule and using the interatomic distance of Mg and Na in the solid, we have .8 Å for the radius of Al^{+} and .7 Å for Al^{2+}. It is clear that ions of this size will be unable to pack the same

way as the small .5 Å Al^{3+} ions pack in the α-alumina. It seems unlikely that the larger ions will be able to fit into the holes in the close-packed oxygen lattice at all. If the valency of the aluminum cation is reduced in the aluminum rich surface layer whose chemical composition is closer to Al_2O or AlO than to Al_2O_3, what kind of surface structure would be expected to form?

It is instructive to compare several oxides of the M_2O_3 type which have the same structure as Al_2O_3, such as V_2O_3, Fe_2O_3 and Ti_2O_3. These cations form stable oxides in their 2+ oxidation states as well (VO, FeO and TiO). The oxides of the MO type, however, have face-centered cubic structures. The ratio of the ionic radii $M^{3+}:O^{2-}$ are very similar for all the compounds to that which is found for Al_2O_3 and which is expected for AlO. Both Al_2O (vapor) and AlO (vapor) are stable and are detected in the vapor composition over α-alumina in equilibrium and also during vaporization into vacuum. The other Group III elements are also known to form stable oxides in their higher 3+ oxidation states, Ga_2O_3, In_2O_3, Tl_2O_3, while their vapors contain the monovalent oxides, Ga_2O, In_2O and Tl_2O in large concentrations. The monovalent oxides in Group III of the periodic table, M_2O, appear to be much more stable than the divalent oxide of the MO type (Tl_2O is a stable solid whose thermodynamic properties have been measured, although only an x-ray powder pattern is reported). Other stable monovalent oxides such as Li_2O and Na_2O which should have smaller ion ratios as in Al_2O form cubic structures of the fluorite type.

Thus it appears that if the high temperature oxygen deficient rotated ($\sqrt{31} \times \sqrt{31}$) surface structure has a composition which

corresponds to Al_2O or AlO, it would be likely to form a cubic overlayer in which the cation is appreciably larger than in the underlying hexagonal (0001) substrate. Strong mismatch due to the differences in structure and ion sizes in the two layers should be expected.

We have been able to generate the rotated $(\sqrt{31} \times \sqrt{31})$ surface structure by placing a cubic overlayer in which the interatomic distance was increased to adjust for the increased cation radius on top of the (0001) substrate. There are several cubic structures which can generate the rotated $(\sqrt{31} \times \sqrt{31})$ unit mesh by coincidence with the (0001) substrate. One of these surface structures is given in Fig. 17.

Additional evidence that the $(\sqrt{31} \times \sqrt{31})$ structure is due to reduced aluminum oxide overlayer comes from studies of the epitaxial deposition of silicon on the (0001) face. Silicon was found to etch the α-alumina surfaces efficiently. Silicon, however, is also a reducing agent which could remove oxygen from the surface by the postulated reaction $Al_2O_3 + 2Si(vapor) = Al_2O + SiO(vapor)$ in addition to the reaction proposed by Chang.[8] It should be noted that the reduced oxides Al_2O, AlO and O and Al are all among the products of the dissociative vaporization of alumina. It was found that silicon causes the formation of the rotated $(\sqrt{31} \times \sqrt{31})$ surface structure above 900°C at temperatures too low for this phase transformation in vacuum. Additional evidence that the rotated $(\sqrt{31} \times \sqrt{31})$ surface structure is composed of a cubic layer on the hexagonal (0001) substrate comes from studies of aluminum oxide structures which are formed on the aluminum metal surface. The oxide has a cubic structure in this aluminum rich environment.

So far we have considered the rotated ($\sqrt{31} \times \sqrt{31}$) structure as a two-dimensional surface structure which forms due to the composition change in the topmost atomic layers at the (0001) face of α-alumina. The possibility that these structural changes are not restricted to the surface layer but are propagated into the bulk of the solid cannot be overlooked. It is unlikely, however, that the oxygen deficient structure could be present in more than a few atomic layers in the bulk. Since oxygen has to be removed to affect the surface rearrangement this would make the rate of bulk rearrangement oxygen diffusion limited. Thus this process would be markedly decelerated as the thickness of the oxygen deficient layer increases. If the reduced oxides of aluminum, Al_2O and AlO, are stable in the α-alumina surface at elevated temperatures, it is likely that the other Group III oxides of the M_2O type might also be stable in the surface environment. Investigation of the surface structures of Ga_2O_3 and In_2O_3 would be of interest. It is also likely that oxides of other metals, MgO and BaO, for example, may have unusual oxidation states which are stabilized in the surface environment. It should be noted that vanadium pentoxide V_2O_5 has been reported recently to undergo a change of surface composition accompanied by loss of oxygen upon heating in vacuum with a corresponding order-order transformation of its surface structure.

X. THE SURFACE CHEMISTRY OF SiO_2 (QUARTZ)

SiO_2 is an unusual material because of the number of phase transformations it undergoes as a function of temperature below its melting point. Each silicon atom is normally bound to 4 oxygen atoms in the SiO_2 structure. However, the tetrahedra so formed can point in different directions with little change in the energy of the structure. It is thus not surprising that a number of specific phases may exist as a function of temperature. The most important phase is the one which is stable at room temperature, α-quartz. Another phase, the β-quartz, which differs little in structure from the α-phase becomes stable above 573°C. The change from α-quartz to β-quartz is very rapid at the transition temperature. If the β-phase is heated to a high temperature of 1400°C a slow transition occurs into a glassy phase. The rate of this transition is a strong function of temperature. A LEED pattern has been obtained from the hexagonal (0001) face of quartz. This is shown in Figure 18. I. Janossy and M. Menyhard[11] have also observed a diffraction pattern on this face. If the crystal is cycled through the transition temperature of 573°C where the α-β transition occurs, no apparent change occurs in the diffraction pattern. The crystal, however, often cracks during this heat treatment. This appears to be due to the volume change which accompanies the α-β transition. If the crystal is heated to high temperatures (above 1000°C) the diffraction pattern slowly disappears, presumably due to the formation of the disordered glassy structure at the surface. Janossy and Menyhard found that the diffraction pattern disappears at a lower temperature (500°C), however.

XI. THE SURFACE CHEMISTRY OF NaF, LiF, AND NaCl (100) FACE

All three alkali halides, NaF, LiF, and NaCl, show no change in diffraction pattern as they are heated to the highest studied temperature, ~ 800°C for LiF, ~ 850°C for NaF, and 400°C for NaCl, that is sufficient to evaporate microscopic amounts of material onto a nearby metal surface with the experimental times of 10-30 minutes. The crystals were in general prepared by cleaving them just before placing them into the vacuum system. The diffraction pattern was visible and after this treatment exhibited the usual (1x1) surface structure. The pattern improved greatly, however, as the crystals were heated to within 200°C of the temperature indicated above, where evaporation became rapid (a monolayer/sec, approximately). This is most likely due to the cleaning of the surface by vaporization that removed the surface contaminants that are volatile at this higher temperature. It appears that the (100) surfaces of these alkali halides maintain a surface structure that is characterisitc of the bulk unit cell at higher temperatures as well as lower temperatures. Unlike alumina and quartz, alkali halides do not undergo surface phase transformations or changes of surface composition.

XII. THE EFFECT OF THE INCIDENT ELECTRON BEAM ON THE SURFACE STRUCTURE OF α-ALUMINA

It was shown that alkali-halides decompose in the incident electron beam, and since the decomposition is rapid, results in a detected decrease of the intensity of the diffraction beams back-scattered from the single crystal surfaces. Aluminum oxide, on the other hand, did not seem to decompose visibly in the electron beam even when the low energy electron beam was allowed to impinge on the crystal for long periods of time (hours). The only indication that the surface chemical composition might change under electron bombardment is when the crystal developed a $(\sqrt{31} \times \sqrt{31})$ surface structure after several hours of electron bombardment using a high current high voltage electron gun (100 μamp at 2000 eV) focused to a small 1 mm^2 spot on the crystal surface. Charig[12] has also found that the $(\sqrt{31} \times \sqrt{31})$ surface structure forms at rather low temperatures (900°C) in the presence of the electron beam. The differences in the decomposition rates of the surfaces between alkali halides and alumina arise from differences in their chemistry. In alkali-halides the diffusion of ions and defects is rather rapid as indicated by the rapid annealing of the surface damage when the alkali halide crystals are heated to moderate temperatures. In alumina surfaces, however, the diffusion of either the aluminum or oxygen or lattice defects appears to be very slow at the temperatures used in this study (up to 1200°C).

Table 1.

NaF Data

Spot Angle	Spot Index	Intensity Data #1	#2	#3	#4	Average Intensity	Average Voltage
9°	00	standard (set at 1.00)				1.00	86
20°	00	.47	.31	.42		.40	82
25°	00	.30	.14	.34		.26	84
30°	00	.13	.14	.21		.16	91
9°	00	.82	.86	.60	.76	.76	141
20°	00	.22	.39	.19		.26	148
25°	00	.13	.08	.16		.09	160
30°	00	.17	.09	.06		.10	158
9°	00	.66	.40	.35		.47	216
20°	00	.19	.17	.13		.16	225
32°	11	.17	.10	.21	.19	.17	101
24°	11	.10	.10	.13	.12	.14	164
44°	20	.10	.12	.27	.24	.18	116
37°	20	.02	.08	.07	.11	.07	176
24°	22	.08	.06	.11		.08	177
20°	10	.04	.04	.06		.05	113
21°	10	.03	.04			.04	121
11°	10	.04	.06	.06		.05	116
26°	21	.02	.03	.04		.03	146
13°	21	.02	< .04	< .04		~.03	205
42°	32	.03	< .04	< .04		~.03	185

Table 1 (continued)

LiF Data

Spot Angle	Spot Index	Intensity Data #1	#2	#3	#4	Average Intensity	Average Voltage
10°	00	standard (set at 1.00)				1.00	125
10°	00	.40	.41	.28	.36	.36	210
10°	00	.38	.44	.46		.46	308
15°	00	.46	.74	1.08		.75	123
15°	00	.20	.33	.16		.25	206
20°	00	.46	.65	.48		.53	122
20°	00	.24	.18	.14	.17	.18	202
33°	11	.27	.23	.22	.29	.25	132
27°	11	.19	.15			.17	220
35°	10	.13	.19	.33		.22	82
23°	10	.46	.31	.53		.43	158
42°	21	.89	.51	.42	.36	.42	180

Note: The angle is the angle of the ray forming the spot to the surface normal. The notation used for th index is LEED notation. In this notation 00, 11, 20, 22 are all even indices; 10, 21, 32 are odd indices.

Table 2.

Ratio of surface Debye temperature to bulk Debye temperature for several elements.

Pb	.47	Reference 13
Pd	.52	"
Bi	.41	"
Ag	.69	"

ACKNOWLEDGMENTS

My deepest and most sincere gratitude is extended to Professor Gabor A. Somorjai whose seemingly boundless energy and encouragement have constantly inspired me during my graduate studies. I wish to extend my appreciation to the Department of Chemistry and the Inorganic Materials Research Division of the Lawrence Berkeley Laboratory of the University of California who have provided me with: (1) an almost perfect graduate student environment, and (2) teaching and research assistantships, respectively, to keep body and soul together during my residence here in Berkeley. Virtually every member of my research group is entitled to some commendation for kindnesses to me, but I wish to express special gratitude to: United States Navy Lt. Commander Hyland B. Lyon, Jr., whose early guidance was most helpful; Helen H. Farrell, whose personal help and kindness even overshadow her tremendous scientific contributions to my work; J. Gordon Davy, Whalun Szeto, and Dan Howlett for their help in solving those endless experimental snags. Special thanks are also extended to Claudia Redwood, Nancy Monroe and the entire staff for their help in the preparation of publications and this dissertation. To Duane Newhart and Emery Kozak I can only express my regrets...that two such master craftsmen (and very nice guys) may not be found anywhere else in this country.

My research was performed under the auspices of the United States Atomic Energy Commission.

REFERENCES

1. C. B. Duke and C. W. Tucker Jr., Surface Sci. 15, 245 (1969).

2. M. Prutton, I. G. Higginbotom, T. E. Gallon, Surface Sci. 21(2), 233 (1970).

3. P. W. Palmberg and T. N. Rhodin, J. Phys. Chem. Solids 29, 1917 (1968).

4. C. B. Duke and C. W. Tucker, Surface Sci. 15, 231 (1969).

5. L. W. Barr, J. Chem. Phys. 51, 1683 (1969).

6. Frederick C. Brown, "The Physics of Solids, Ionic Crystal Lattice Vibrations, and Imperfections," (Benjamin, New York, 1967), p. 303.

7. C. C. Chang, J. Appl. Phys. 39, 5570 (1968).

8. C. C. Chang, "Proceedings of the Conference on the Structure and Chemistry of Solid Surfaces," G. A. Somorjai ed., Sect. 77 (Wiley and Sons, New York, 1969).

9. J. M. Charig and D. K. Skinner, "Proceedings of the Conference on the Structure and Chemistry of Solid Surfaces," G. A. Somorjai ed., Sect. 34, (John Wiley and Sons, New York, 1969).

10. L. Pauling, "The Nature of the Chemical Bond," (Cornell University Press, Ithaca, N. Y. 1960).

11. I. Janossy and M. Menyhard, Surface Sci. 25, 647 (1971).

12. J. M. Charig, Appl. Phys. Lett. 10, 139 (1967).

13. R. M. Goodman, H. H. Farrell and G. A. Somorjai, J. Chem. Phys. 48, 1046 (1968).

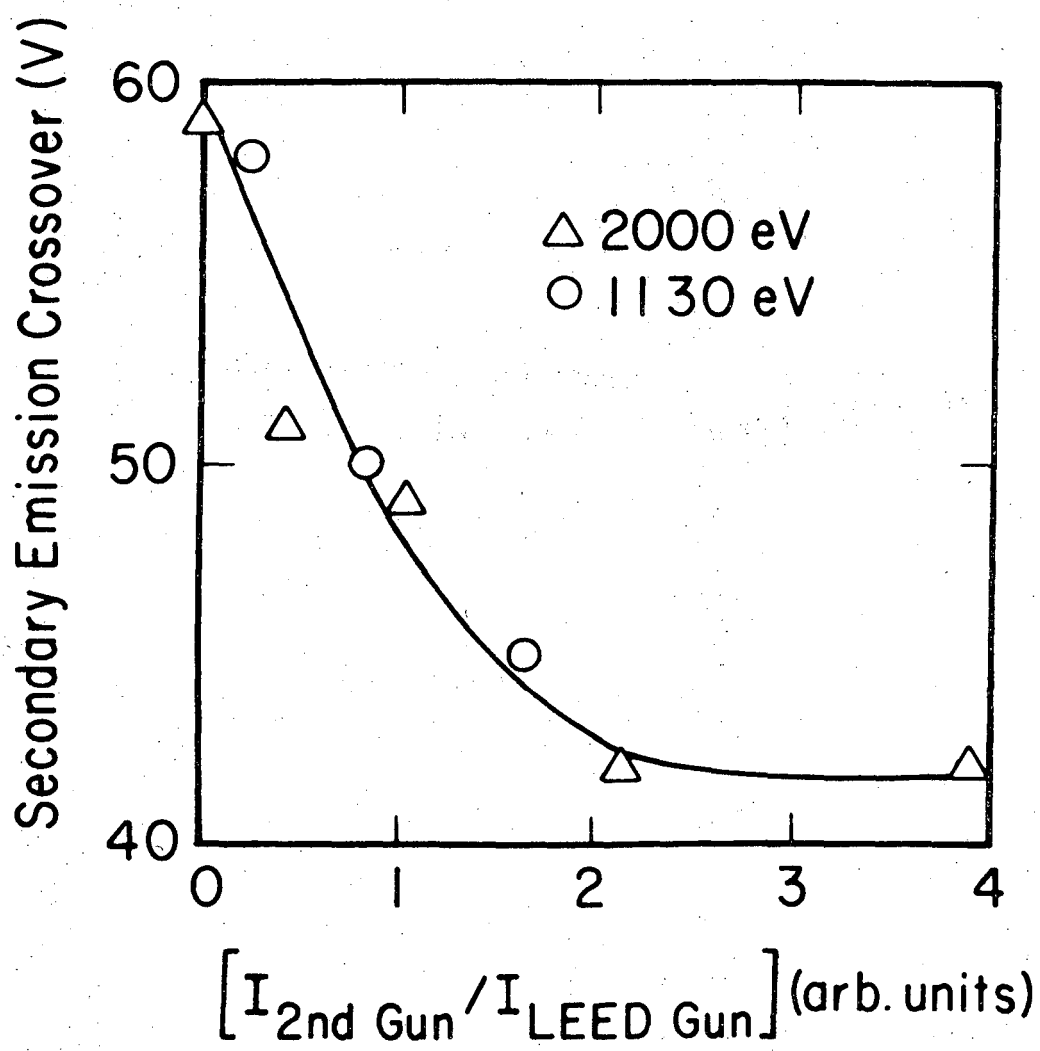

XBL 7111-7536

Fig. (1)

Lowering of the secondary emission crossover of Al_2O_3(0001) surface by means of second electron gun set at grazing angle.

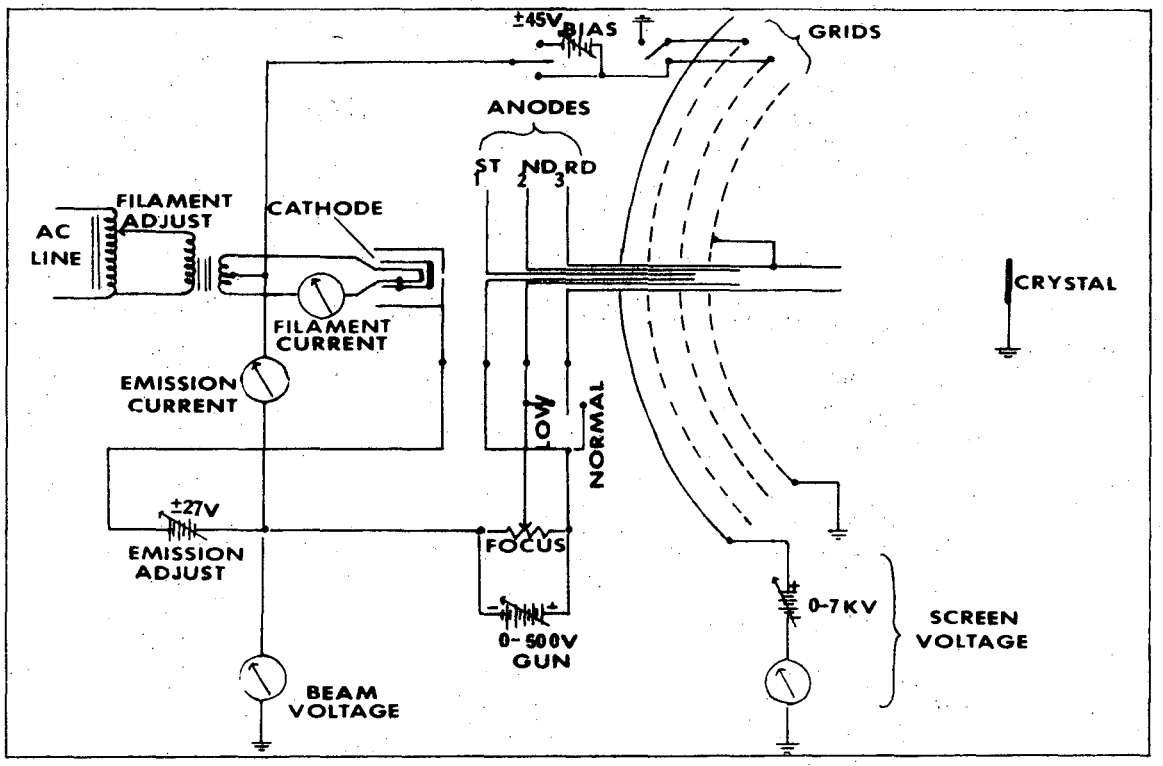

LEED ELECTRON OPTICS

XBL 696-632

Fig. (2)

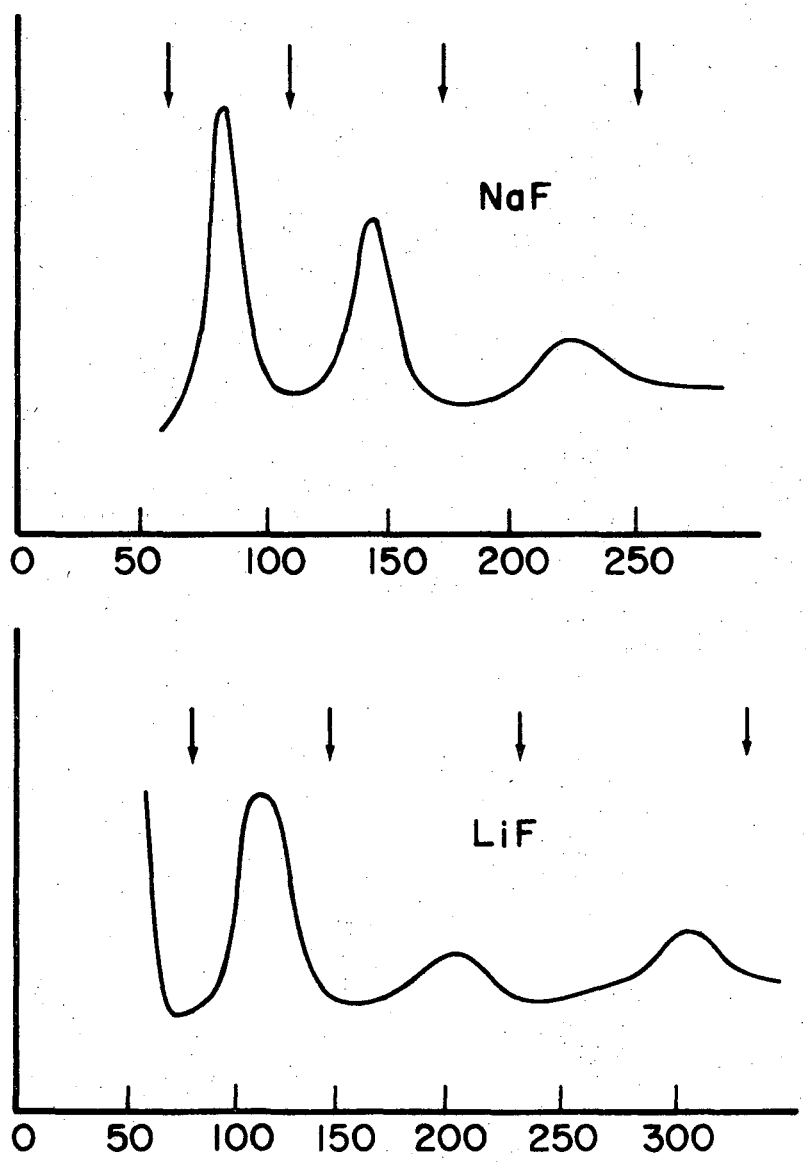

XBL 718-7189

Fig. (3)

I_{oo} vs. voltage, arrows indicate calculated maxima with no correction for surface charge or inner potential.

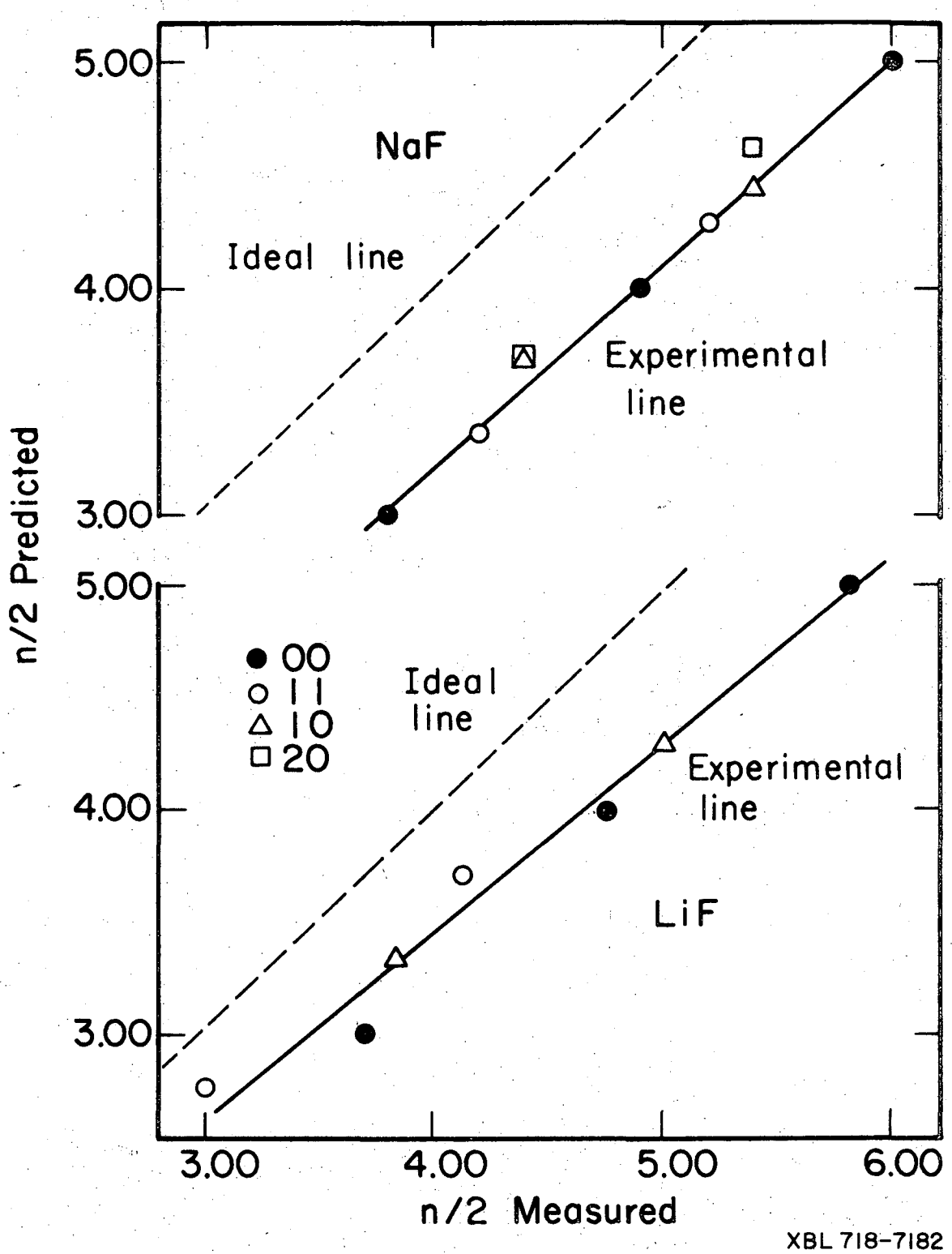
5.00
4.00
3.00
NaF
Ideal line
Experimental line
5.00
4.00
3.00
00
11
10
20
Ideal line
Experimental line
LiF
n/2 Predicted
3.00
4.00
5.00
6.00
n/2 Measured
XBL 718-7182

Fig. (4)

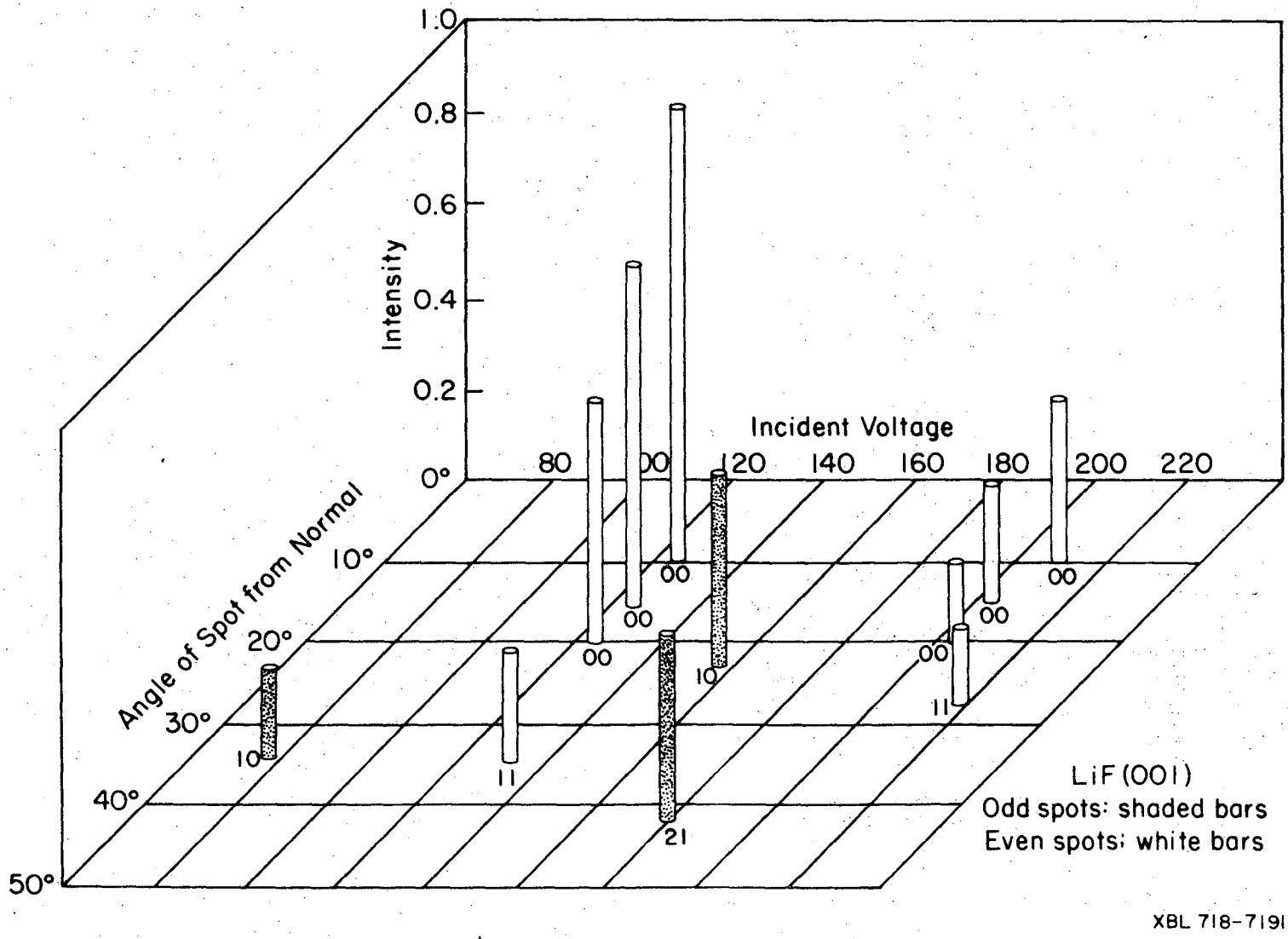
1.0
0.8
0.6
0.4
0.2
0°
Intensity
Incident Voltage
80
100
120
140
160
180
200
220
Angle of Spot from Normal
10°
20°
30°
40°
50°
00
00
00
10
11
21
10
00
00
00
11
LiF (001)
Odd spots: shaded bars
Even spots: white bars
XBL 718-7191

Fig. (5)

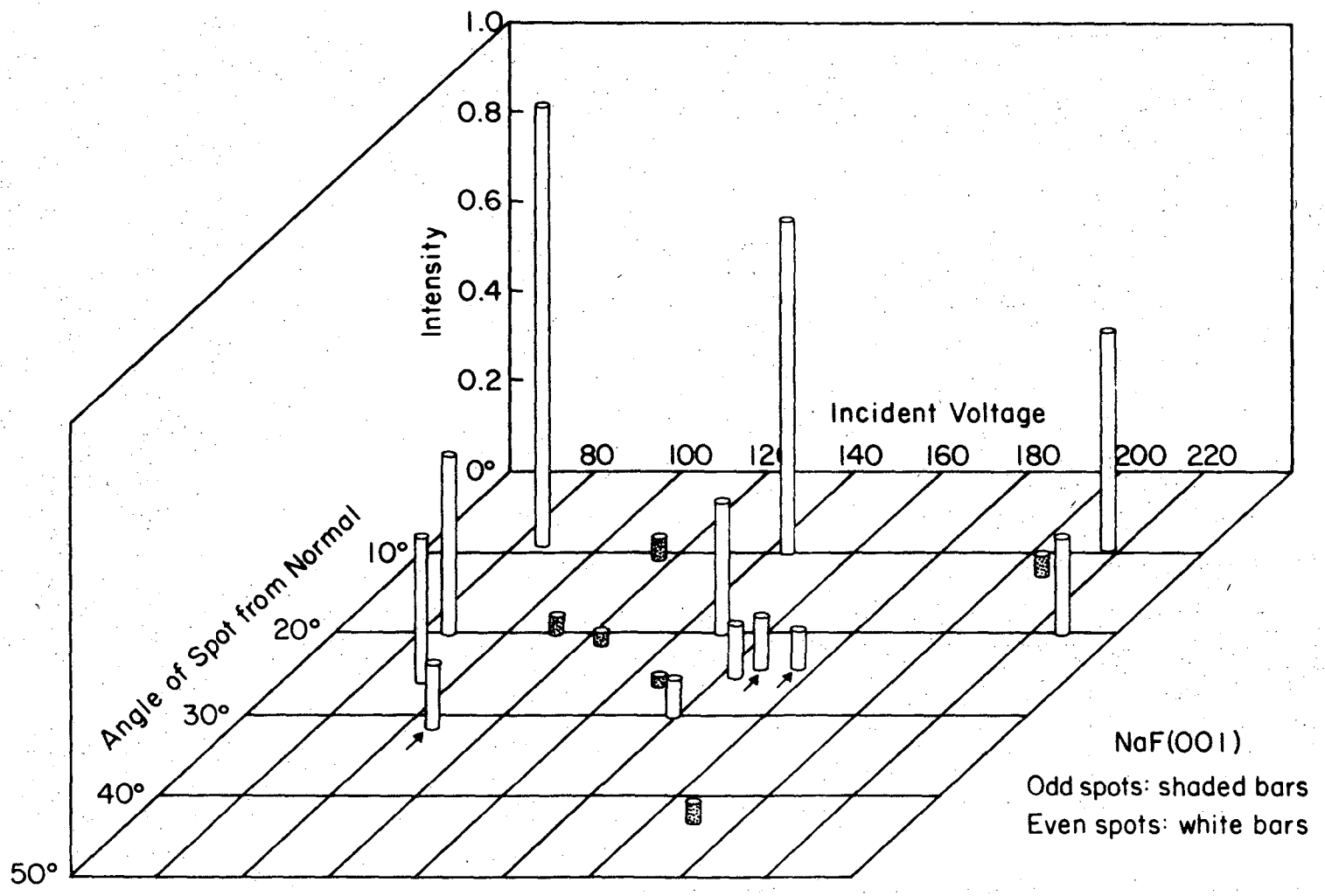

XBL 718-7190

Fig. (6)

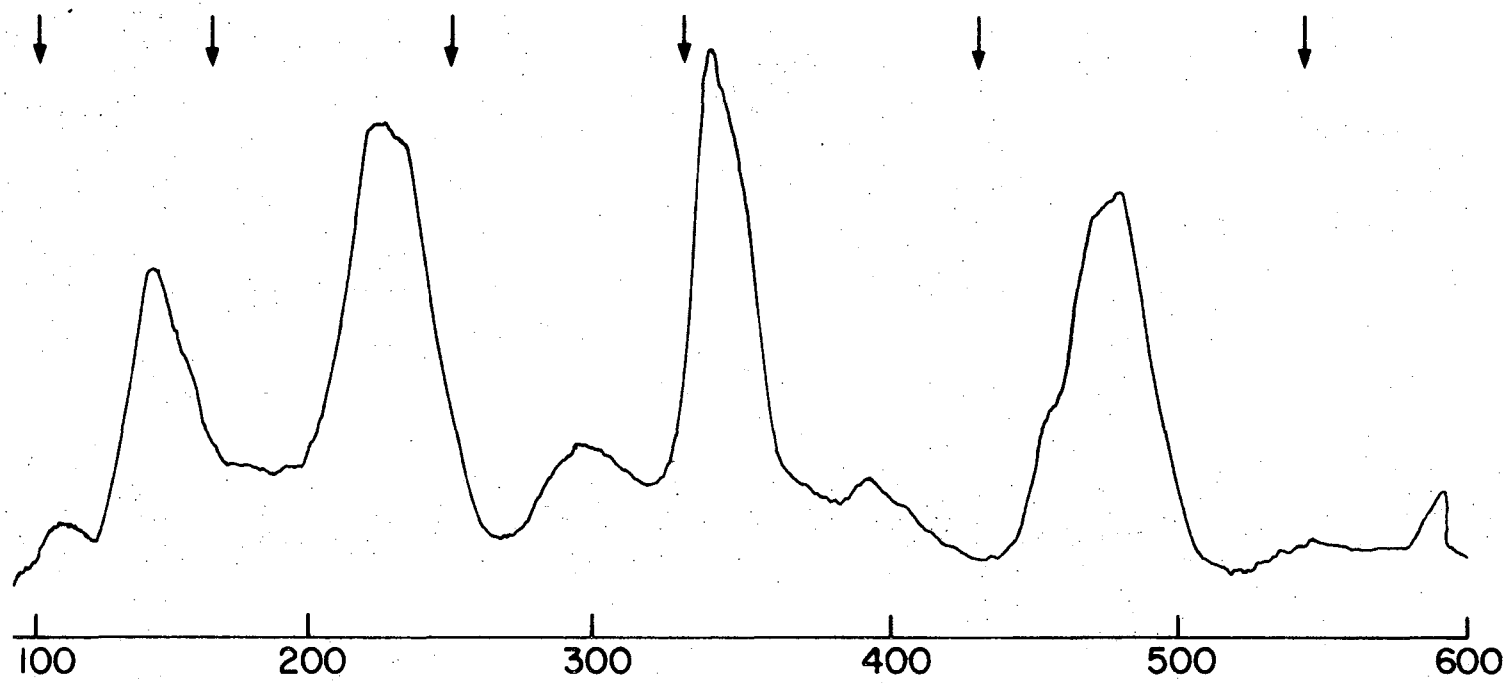

XBL 718-7184

Fig. (7)

Al_2O_3 (0001) 1X1 surface I_{oo} vs. eV 5° incident angle--arrows indicate positions of kinematic maxima; no correction is made for surface charge.

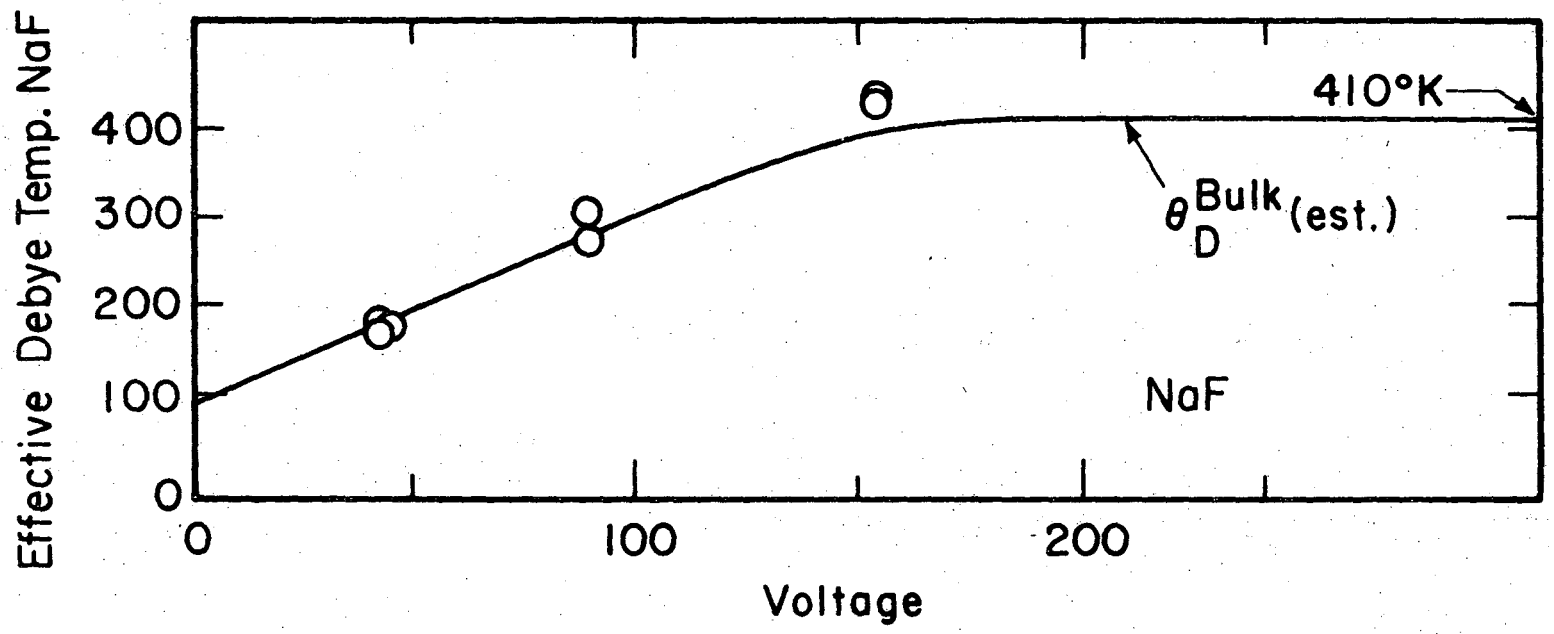

XBL 716-6855

Fig. (8)

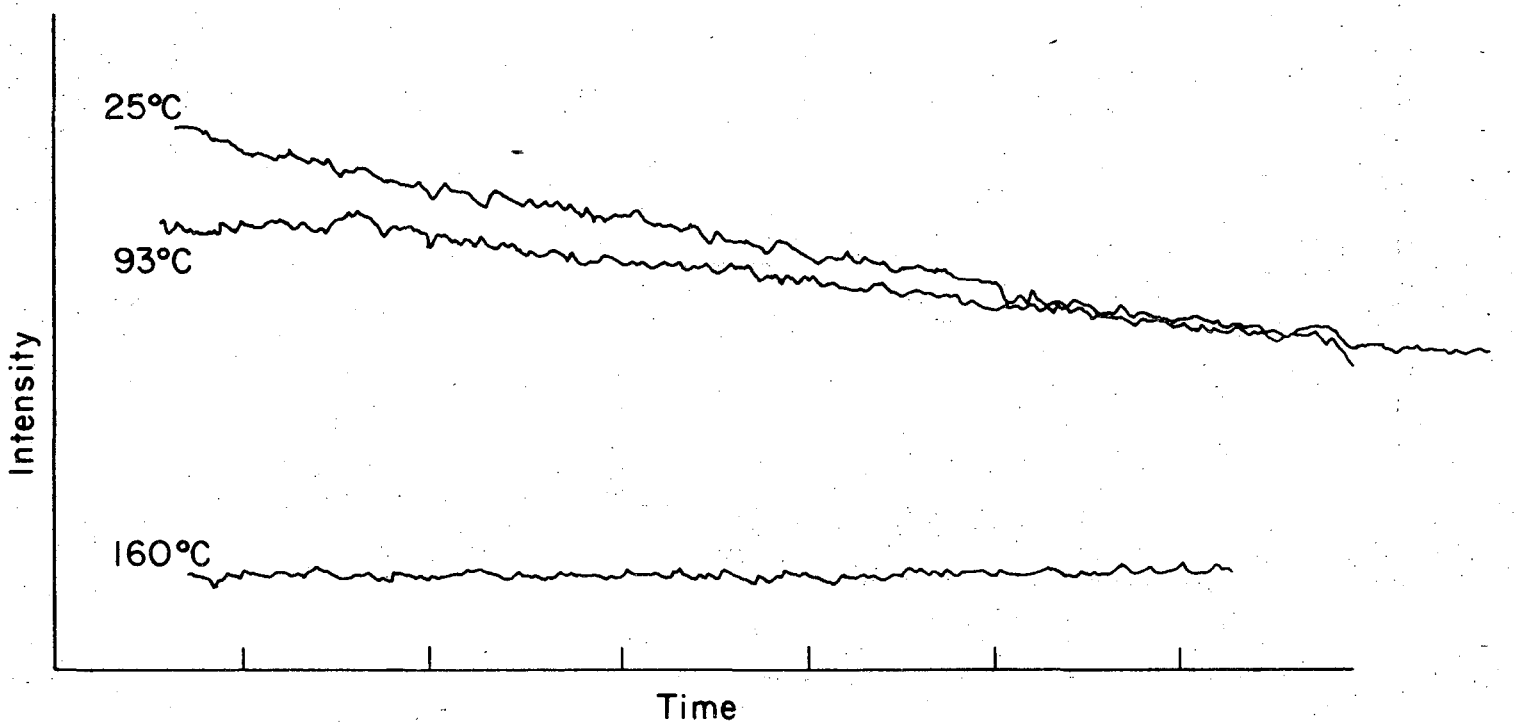

XBL 718-7186

Fig. (9)
Decomposition of NaF(100) as a function of time.

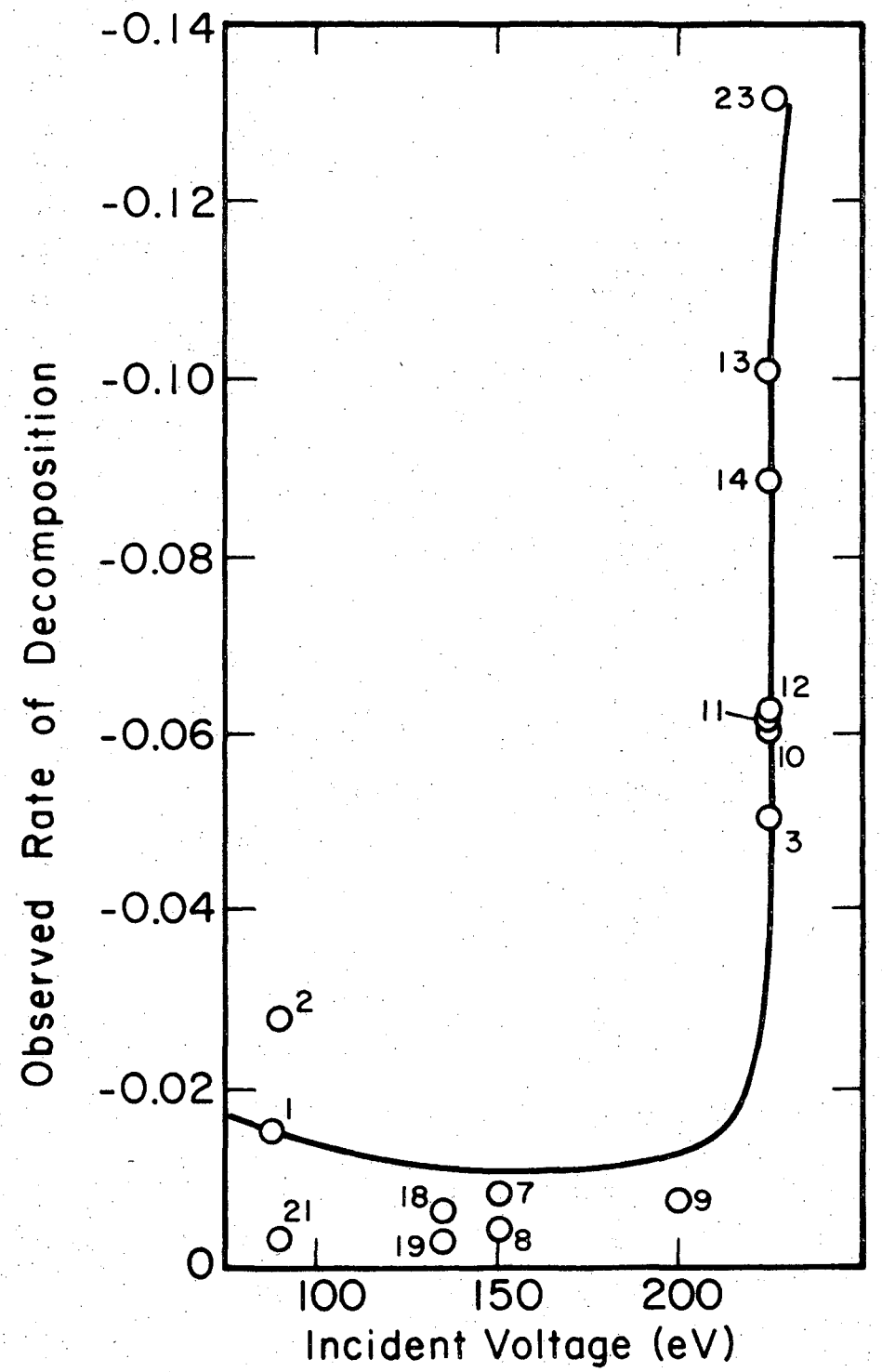

XBL 718-7188

Fig. (10)

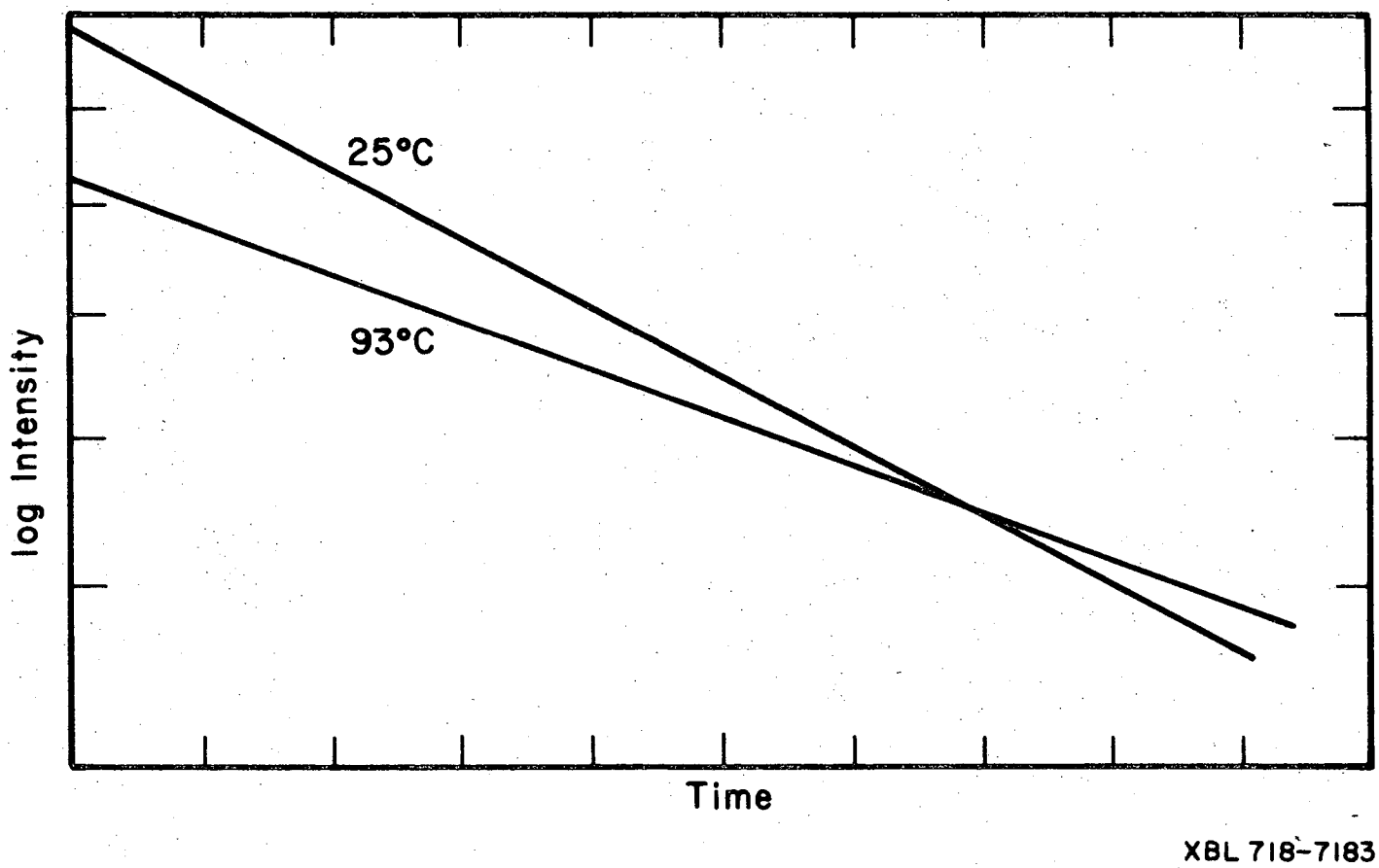

Fig. (11)

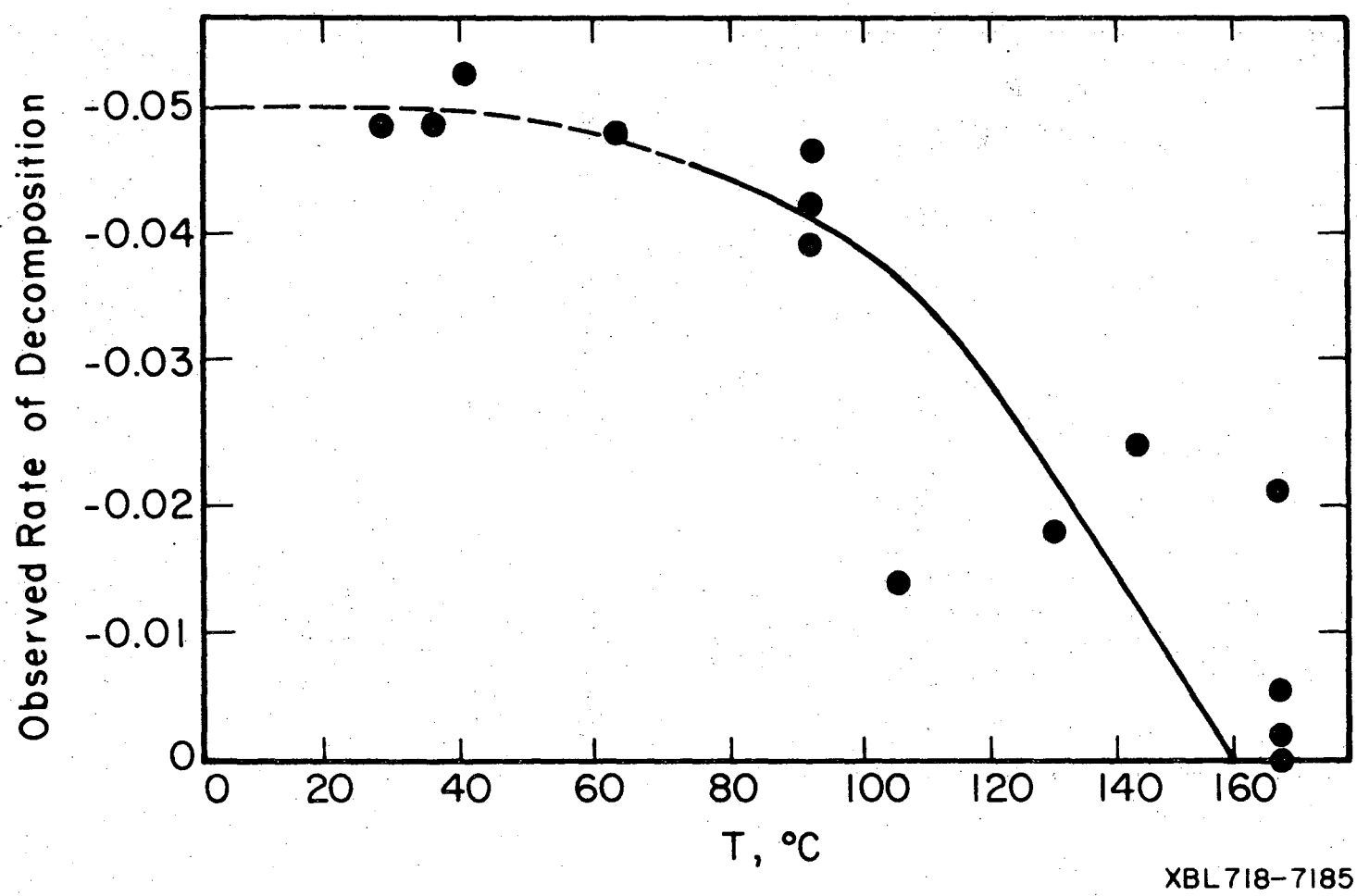
Observed Rate of Decomposition
-0.05
-0.04
-0.03
-0.02
-0.01
0
0
20
40
60
80
100
120
140
160
T, °C
XBL718-7185

Fig. (12)

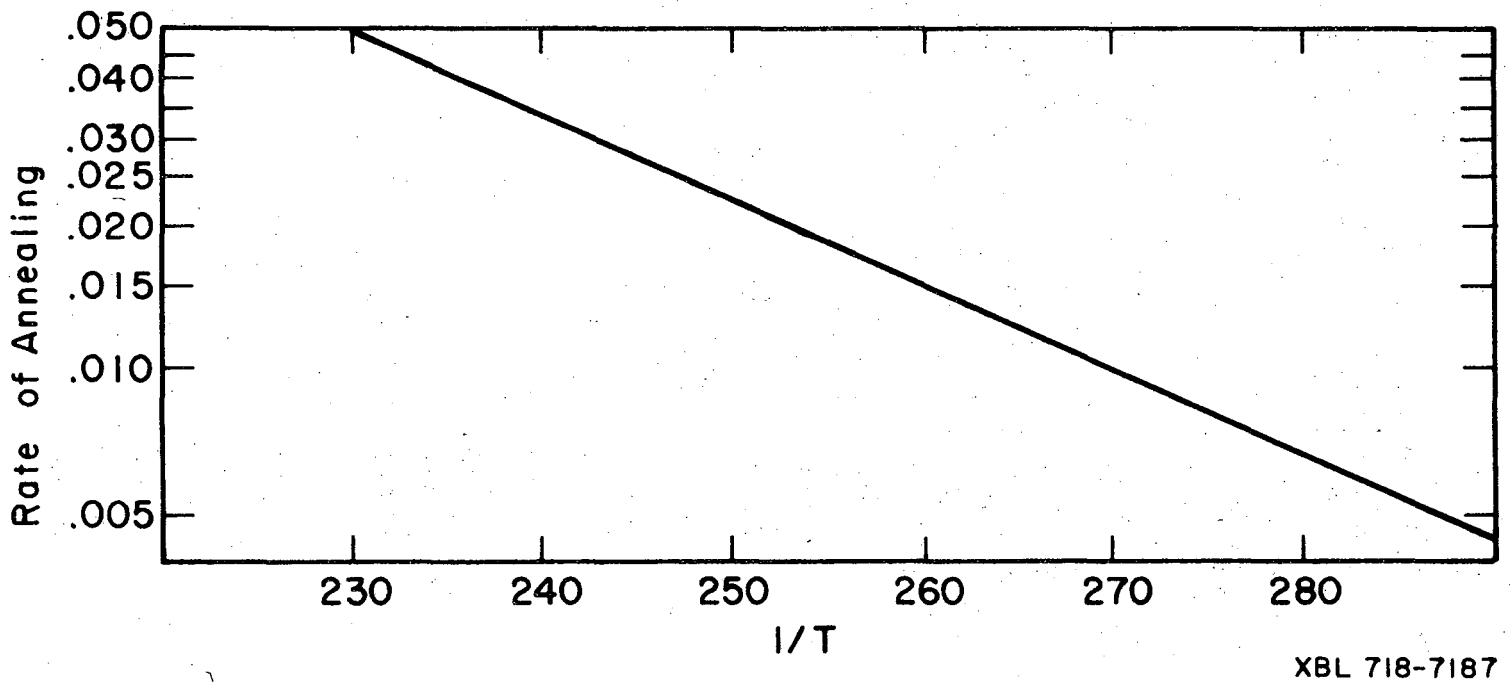
.050
.040
.030
.025
.020
.015
.010
.005
Rate of Annealing
230
240
250
260
270
280
1/T
XBL 718-7187

Fig. (13)

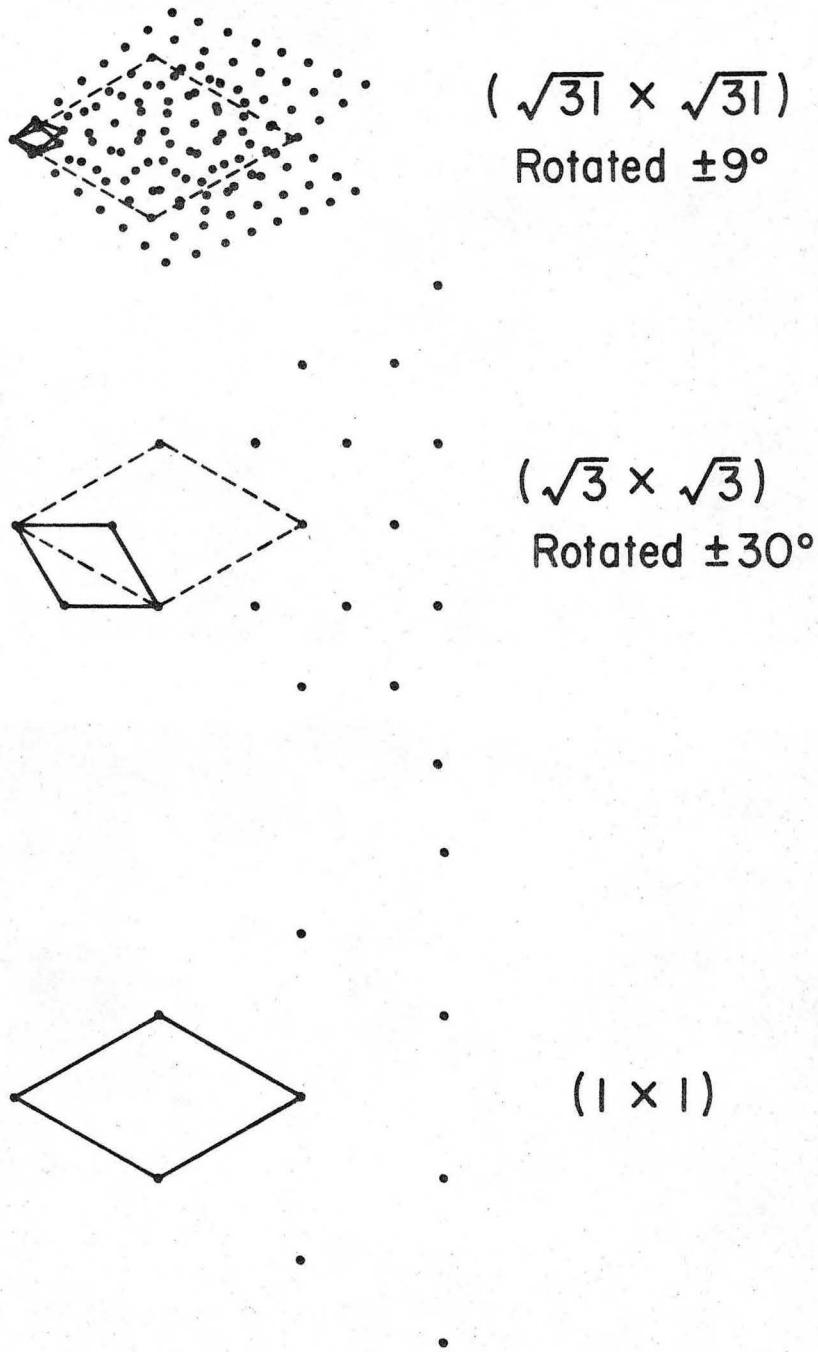

XBL 701-5

Fig. (14)

Schematic representation of three aluminum oxide diffraction patterns which are due to the appearance of different surface structures on the (0001) crystal face.

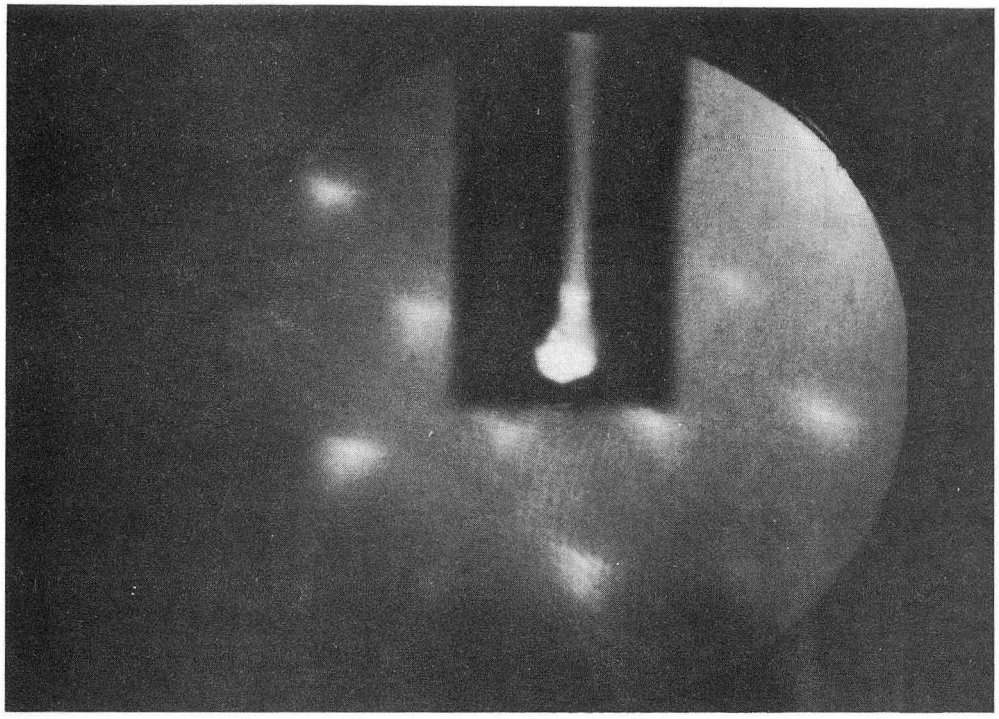

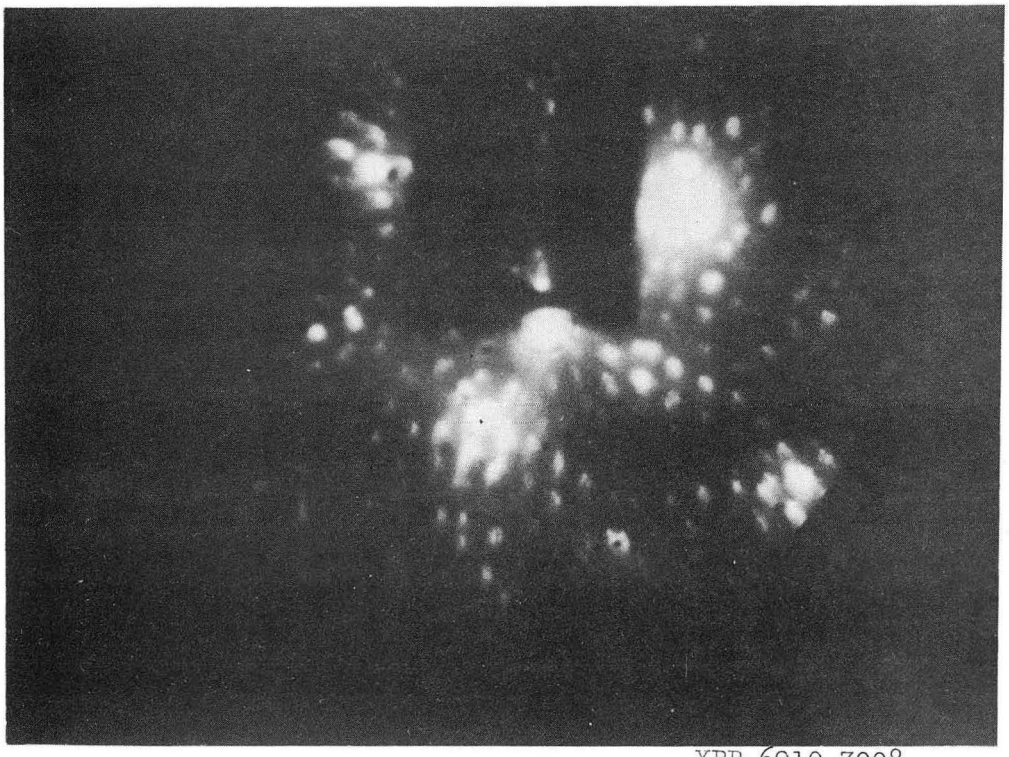

XBB 6910-7008

Fig. (15)

($\sqrt{31}$ X $\sqrt{31}$) diffraction pattern from the Al_2O_3 (0001) surface

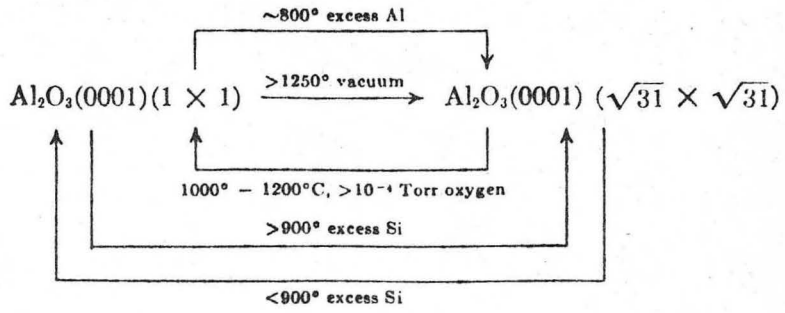

Fig. (16)

Chemical changes on the Al_2O_3 surfaces and their characteristic conditions

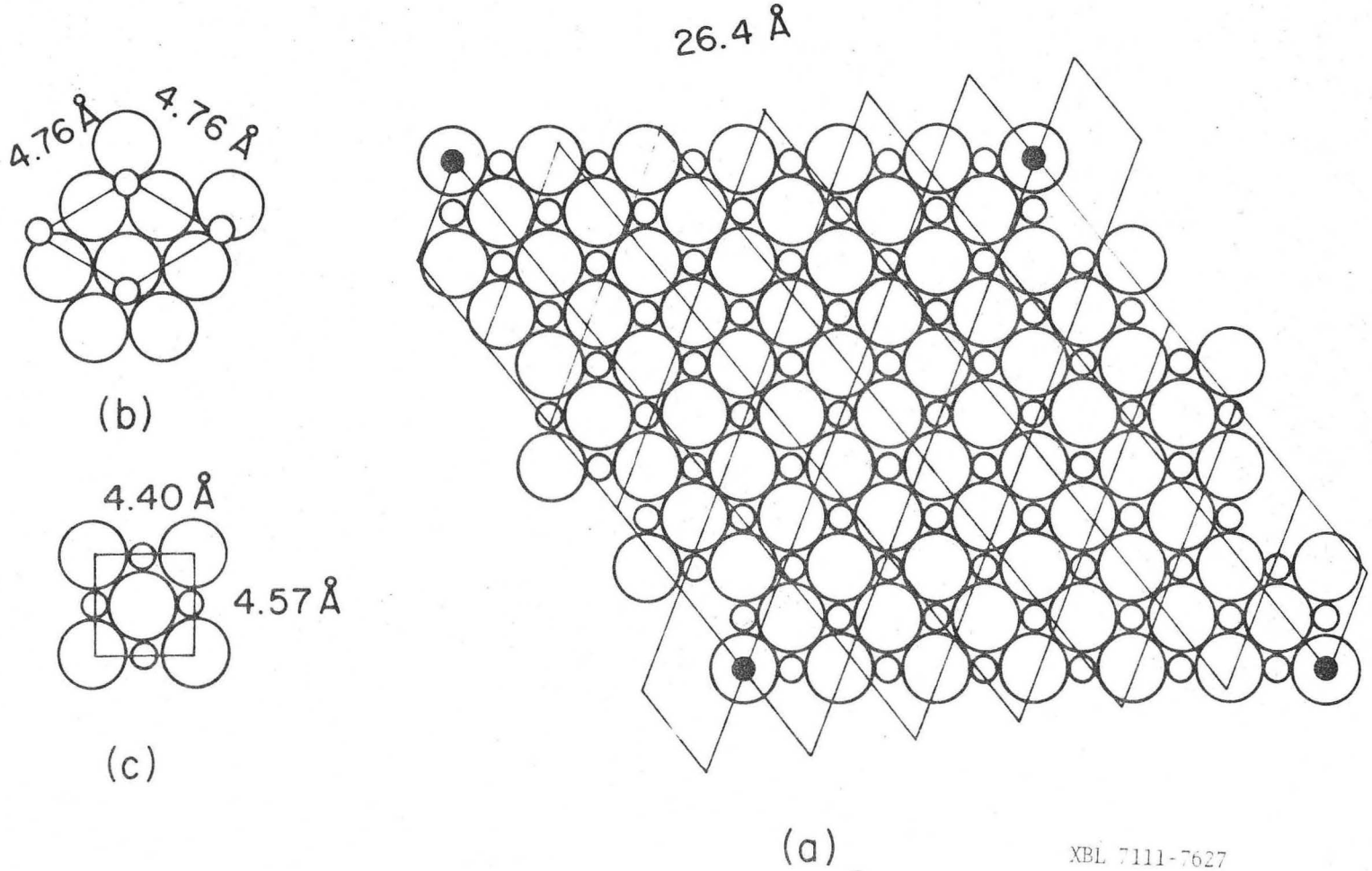

XBL 7111-7627

Fig. (17)

(a) Possible structure on the surface of Al_2O_3(0001) ($\sqrt{31}$ X $\sqrt{31}$) (b) Unit cell of substrate atoms which form pattern a (c) Unit cell of square AlO overlay which is superimposed upon b to generate the structure in a.

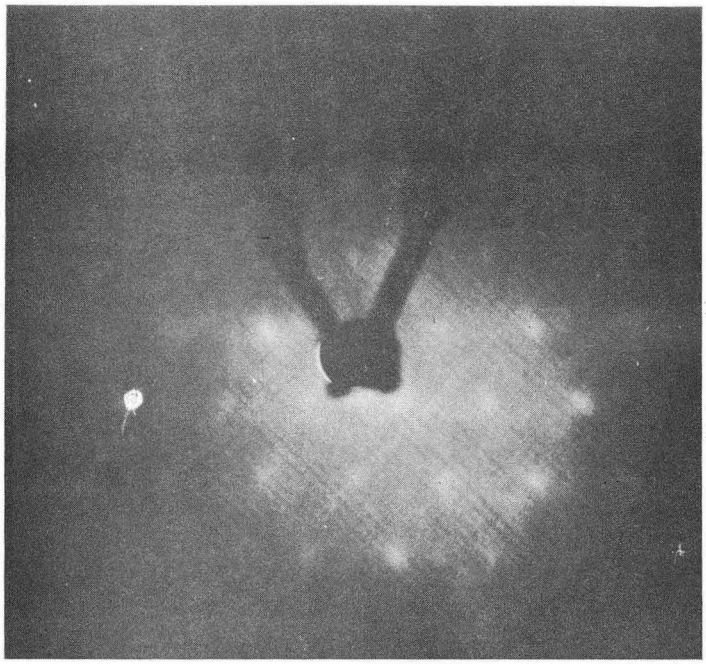

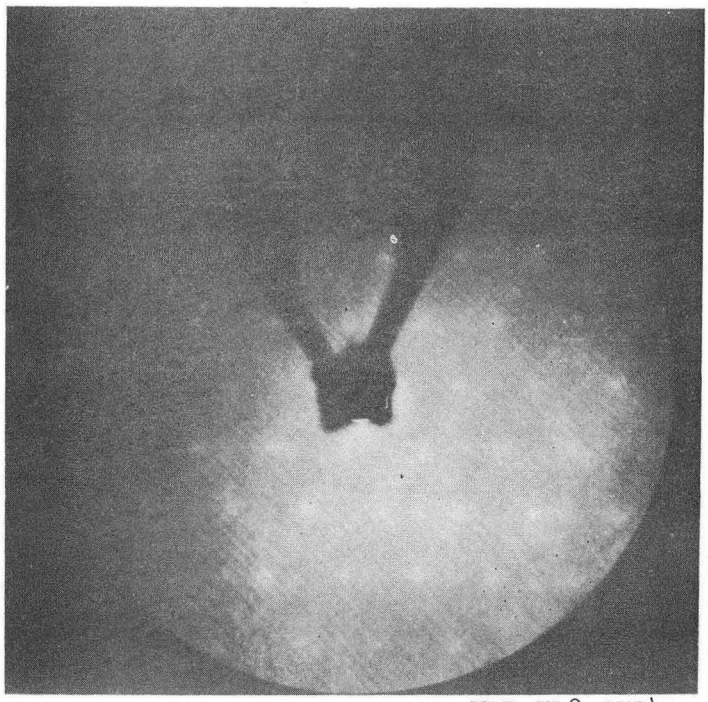

XBB 718-3734

Fig. (18)

SiO_2 diffraction pattern 150 eV top;

212 eV bottom

LEGAL NOTICE

This report was prepared as an account of work sponsored by the United States Government. Neither the United States nor the United States Atomic Energy Commission, nor any of their employees, nor any of their contractors, subcontractors, or their employees, makes any warranty, express or implied, or assumes any legal liability or responsibility for the accuracy, completeness or usefulness of any information, apparatus, product or process disclosed, or represents that its use would not infringe privately owned rights.

TECHNICAL INFORMATION DIVISION
LAWRENCE BERKELEY LABORATORY
UNIVERSITY OF CALIFORNIA
BERKELEY, CALIFORNIA 94720